AFRL-RV-PS-
TR- 2018-0097

AFRL-RV-PS-
TR- 2018-0097

EXPERIMENTAL SOLAR ARRAY SPACE FLIGHT TEST ON THE AFRL TacSat-2 SPACECRAFT

Paul Hausgen, et al.

4 June 2018

Interim Report

APPROVED FOR PUBLIC RELEASE; DISTRIBUTION IS UNLIMITED.

AIR FORCE RESEARCH LABORATORY
Space Vehicles Directorate
3550 Aberdeen Ave SE
AIR FORCE MATERIEL COMMAND
KIRTLAND AIR FORCE BASE, NM 87117-5776

DTIC COPY

NOTICE AND SIGNATURE PAGE

AFRL-RV-PS-TR-2018-0097 HAS BEEN REVIEWED AND IS APPROVED FOR PUBLICATION IN ACCORDANCE WITH ASSIGNED DISTRIBUTION STATEMENT.

//signed//	//signed//
JESSICA BUCKNER Program Manager	JOHN BEAUCHEMIN Chief Engineer, Spacecraft Technology Division

Space Vehicles Directorate

REPORT DOCUMENTATION PAGE

Form Approved
OMB No. 0704-0188

1. REPORT DATE *(DD-MM-YYYY)*
04-06-2018

2. REPORT TYPE
Interim Report

3. DATES COVERED *(From - To)*
1 Jan 2018 - 4 Jun 2018

4. TITLE AND SUBTITLE
Experimental Solar Array Space Flight Experiment on the AFRL TacSat-2 Spacecraft

5a. CONTRACT NUMBER

5b. GRANT NUMBER

5c. PROGRAM ELEMENT NUMBER
63401F

6. AUTHOR(S)
Paul E. Hausgen, Bernie Carpenter, and Neeraj Gupta

5d. PROJECT NUMBER
682J

5e. TASK NUMBER
PPM00036720

5f. WORK UNIT NUMBER
EF130335

7. PERFORMING ORGANIZATION NAME(S) AND ADDRESS(ES)
Air Force Research Laboratory
Space Vehicles Directorate
3550 Aberdeen Ave. SE
Kirtland AFB, NM 87117-5776

8. PERFORMING ORGANIZATION REPORT NUMBER
AFRL-RV-PS-TR-2018-0097

9. SPONSORING / MONITORING AGENCY NAME(S) AND ADDRESS(ES)

10. SPONSOR/MONITOR'S ACRONYM(S)
AFRL/RVSV

1 1. SPONSOR/MONITOR'S REPORT NUMBER(S)

12. DISTRIBUTION / AVAILABILITY STATEMENT
Approved for public release; distribution is unlimited. (AFMC-2018-0563. dtd 26 Nov 18)

13. SUPPLEMENTARY NOTES

14. ABSTRACT
This technical report presents the physical configuration, preflight testing, and on-orbit data analysis for the Experimental Solar Array flown on the TacSat-2 satellite (a.k.a. Roadrunner). Successful deployment of the fold integrated thin-film stiffening solar array was demonstrated. In addition, on-orbit electrical performance data was obtained for approximately 79 watts (Beginning-of-Life (BOL), Air Mass 0 (AM0), at 25°C) of triple junction a-Si (amorphous silicon) thin-film solar cells integrated in a series/parallel configuration to support a 28V spacecraft bus. Measured on-orbit electrical data showed reasonable agreement with predicted on-orbit operation.

15. SUBJECT TERMS
a-Si, solar arrays, spacecraft, thin film solar cells, flights programs, lab characterization tools, novel materials, power system, space power, systems, spacecraft, sub-systems

16. SECURITY CLASSIFICATION OF:			17. LIMITATION OF ABSTRACT	18. NUMBER OF PAGES	19a. NAME OF RESPONSIBLE PERSON Jessica Buckner
a. REPORT Unclassified	b. ABSTRACT Unclassified	c. THIS PAGE Unclassified	Unlimited	42	19b. TELEPHONE NUMBER *(include area code)*

Standard Form 298 (Rev. 8-98)
Prescribed by ANSI Std. 239.18

This page is intentionally left blank

TABLE OF CONTENTS

LIST OF FIGURES

LIST OF TABLES

1 SUMMARY

This technical report presents the physical configuration, preflight testing, and on-orbit data analysis for the Experimental Solar Array (ExpSA) flown on the TacSat-2 satellite (a.k.a. Roadrunner). Successful deployment of the Fold Integrated Thin-Film Stiffening (FITS) solar array was demonstrated. In addition, on-orbit electrical performance data was obtained for approximately 79 watts (Beginning-of-Life (BOL), Air Mass 0 (AM0), at 25°C) of triple junction a-Si (amorphous silicon) thin-film solar cells integrated in a series/parallel configuration to support a 28V spacecraft bus. Measured on-orbit electrical data showed reasonable agreement with predicted on-orbit operation.

2 INTRODUCTION

The ExpSA experiment included two deployed solar array wings and an electronics box used to measure the electrical characteristics of the solar array over time. The ExpSA flight experiment included multiple advanced technologies: amorphous silicon (a-Si) flexible, thin-film solar cells, Fold-Integrated Thin-film Stiffening solar array deployment system/support structure, and Elastic Memory Composite (EMC) root hinges. Detailed information regarding these technologies can be found in published technical reports [1], [2], [3]. This report focuses on the on-orbit performance of these technologies. A summary of the ExpSA results has been published in reference [4]. Additional information regarding FITS and ExpSA can be found in [5] and [6].

3 METHODS, ASSUMPTIONS, AND PROCEDURES

3.1 Mission Objectives

The objectives of the Experimental Solar Array flight experiment were to:

1) Verify successful on-orbit deployment of the FITS solar array deployment system developed by Sierra Nevada Corporation (formerly MicroSat Systems, Inc. (MSI))
2) Measure on-orbit performance of a-Si thin-film solar cells manufactured by United Solar Ovonic (USO) Corporation
3) Verify successful deployment of Elastic Memory Composite hinges developed by Composite Technology Development, Inc. (CTD).
4) Provide supplemental power to the TacSat-2 spacecraft bus to support increased payload operation

Objectives (1) and (3) were assessed by optical imagery and comparing the wing power output to the expected value. The on-orbit performance of the a-Si thin-film solar cells (objective 2) was measured by applying an electronic load on a periodic basis to generate current/voltage curves. Objective 4 was assessed by examining spacecraft telemetry (total solar array current) when the ExpSA strings were switched into the spacecraft bus.

3.2 Experimental Approach

The ExpSA experiment was designed to operate in three modes while on-orbit: (1) deployment mode, (2) bus power, and (3) electrical characterization. While in bus power mode, both ExpSA wings were electrically connected to the main spacecraft power bus with the intent of providing supplemental power. On a periodic schedule, the ExpSA wings were switched from the spacecraft bus to an electronic load for electrical performance characterization (current/voltage curves). The nominal state for the ExpSA was the bus power mode.

During the deployment mode, power to the CTD EMC hinge heaters was turned on, and a controller within the ExpSA control electronics (aka IV (current/voltage) box) cycled the heater power to achieve a desired EMC hinge deployment temperature. The elevated temperature was required to release the stored strain energy in the stowed EMC hinges to enforce deployment. Once the required temperature was reached the command was issued from the spacecraft to release the wing deployment restraints.

During bus power mode, the electrical power generated by the ExpSA was made available to the spacecraft bus. In this mode, the power to the IV box was off and the power collected from the ExpSA wings ran through the IV box into the spacecraft IAU (integrated avionics unit). Two relays in the spacecraft IAU switched each ExpSA wing independently onto the spacecraft power bus depending on the battery SOC (state of charge) and the spacecraft bus power load. All solar array strings (including ExpSA) were connected in parallel to the TacSat-2 battery pack. As a result, the load point of each ExpSA wing when connected to the spacecraft power bus was determined by the battery voltage at that point in time.

The spacecraft telemetry was examined carefully to determine the impact of adding the individual ExpSA wings to the spacecraft electrical bus. Bus telemetry included solar array current, which was a summation of all connected strings that were providing current to the battery at any instant in time. The effect of adding the ExpSA wings to the electrical bus was determined by identifying solar array string switch states in which the only switch change involved one of the ExpSA wings and noting the difference in total solar array current (difference is current contribution of ExpSA wing).

The goal of the electrical characterization mode was to monitor the wing electrical performance as a function of time on-orbit. Electrical characterization was achieved using an electronic load that was programmed to generate a fixed number of data points per sweep. The experimental approach involved maintaining a load point for a fixed period of time, measuring the current and voltage produced by the array, and outputting the values as proportional voltages that were read by the main spacecraft avionics on two analog voltage channels. The resulting data set was a stair step of voltage and current pairs, which started at open circuit (zero current), and increased the current in set increments toward short circuit. Each data collect session included multiple current/voltage sweeps.

Given that the electrical performance is highly dependent on temperature, the solar array wing temperature was measured by two PRT (Platinum Resistance Thermometer) sensors that were mounted to the backside of the array. The electrical performance data were corrected to standard measurement conditions (25° C) to allow the on-obit data to be compared to pre-flight measurements.

3.3 Experiment Configuration

The two ExpSA wings were stowed on the backside of the main solar array (one on each wing, see Figure 1). The block diagram of the ExpSA flight experiment is shown in Figure 2. The elements within the block diagram that were provided by the ExpSA team are the IV box and the two a-Si solar array wings. The ExpSA wings were deployed after the main solar array was successfully deployed. The deployed state can be seen in Figure 3.

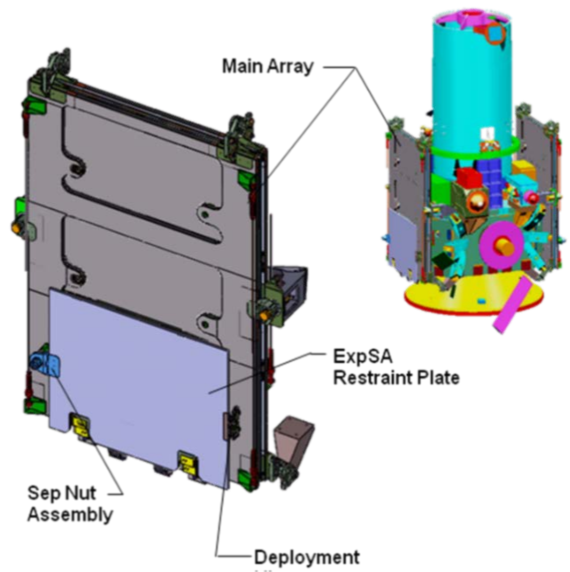

Figure 1. ExpSA Stowed (Removed from TacSat-2 and Mounted on TacSat-2)

3.4 ExpSA Wings

The two ExpSA wings consisted of an innovative structural design that enabled very compact stowage with passive deployment upon launch restraint release (driven by stored strain energy). The structural approach is referred to as FITS and was developed by Sierra Nevada Corporation (formerly MicroSat Systems). Detailed information on the FITS technology is provided in [1] and [2].

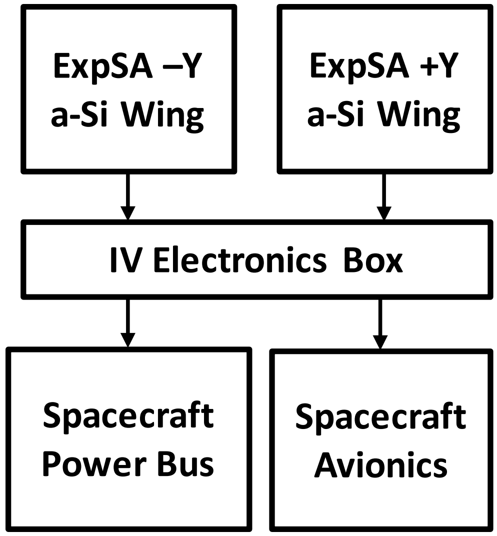

Figure 2. Experimental Solar Array System Block Diagram

The power generation was provided by a-Si flexible thin-film photovoltaics (TFPV) fabricated by United Solar Ovonics [3]. Approximately 79 watts BOL of the a-Si thin film solar cells were assembled into modules and integrated into the FITS solar array wing structure. The a-Si solar cells had thin stainless steel substrates (~1 mil) and were integrated on a Kapton® blanket with copper traces for electrical connection. The solar cell parallel/series arrangement was designed such that it could support a 28 V bus. Figure 4 shows a schematic of the cell layout and dimensions for the individual wings.

Figure 5 shows one of the flight wings during preflight IV (current/voltage) testing. The electrical circuit for one wing is shown in Figure 6. Both wings had an identical electrical layout and the same solar cell technology (a-Si thin-film solar cells).

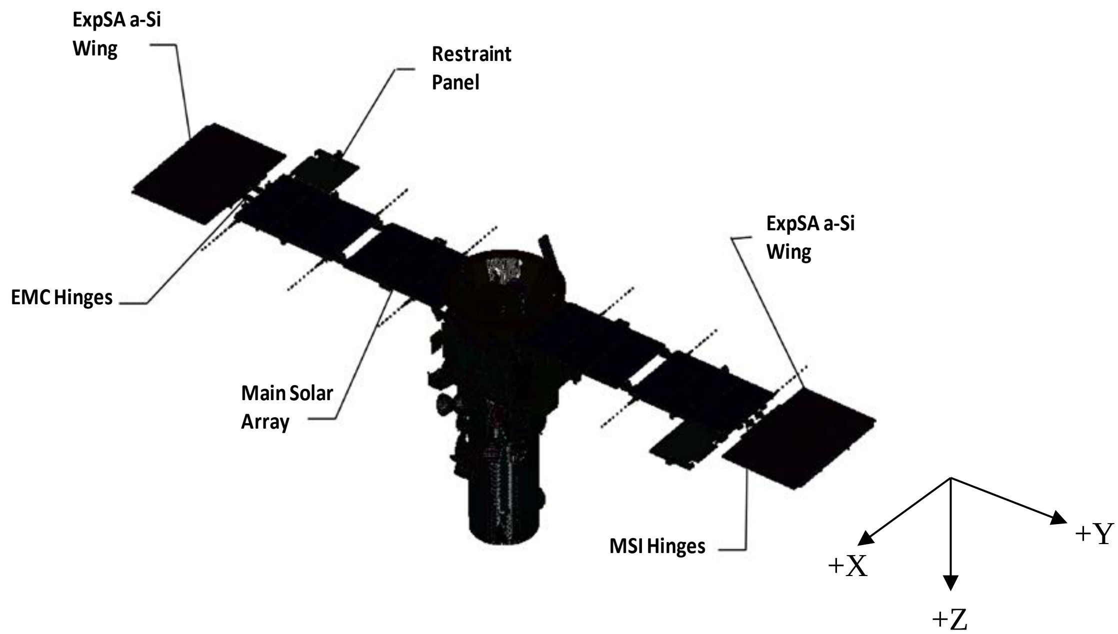

Figure 3. ExpSA Deployed on TacSat 2

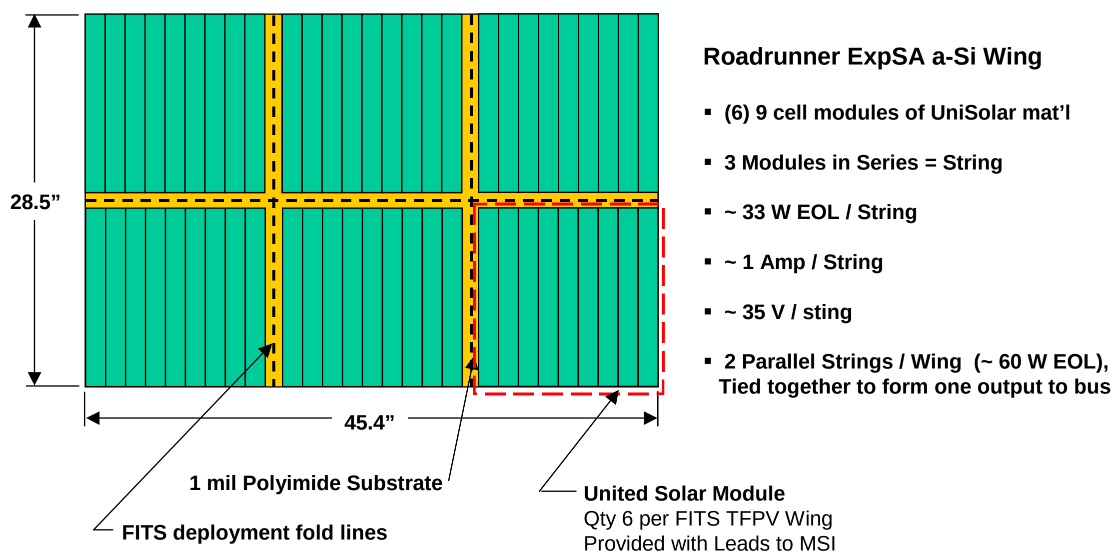

Figure 4. ExpSA a-Si TFPV Blanket Layout (EOL is End of Life)

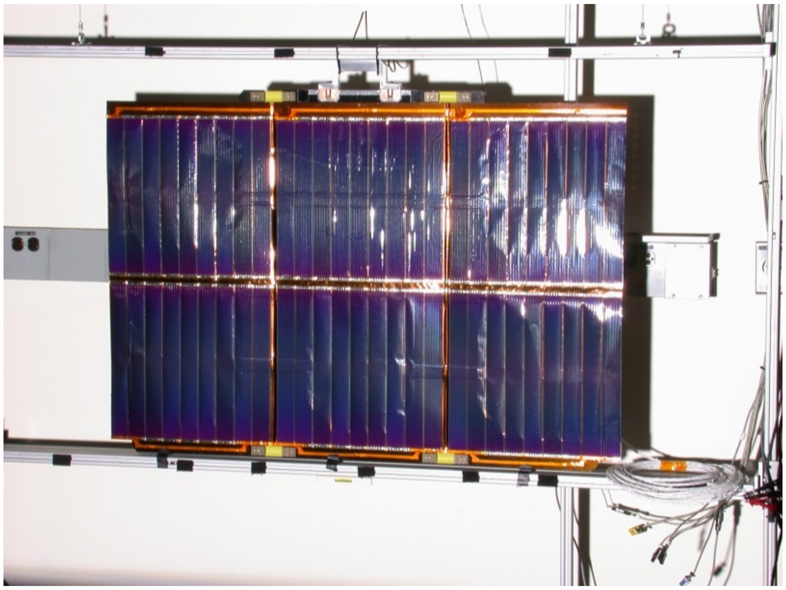

Figure 5. a-Si flight Wing Undergoing Pre-flight Electrical Performance Testing

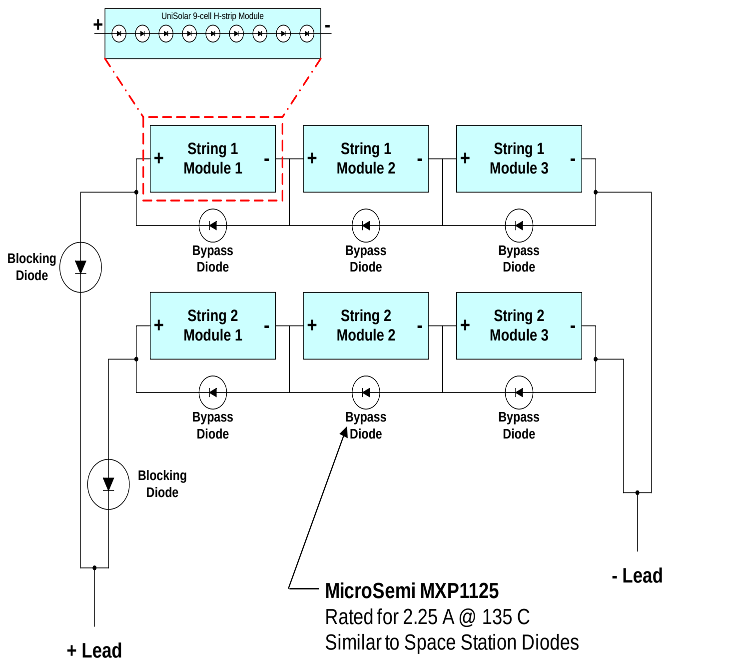

Figure 6. ExpSA Electrical Circuit Layout for One Wing

3.5 Elastic Memory Composite Hinge

The two root hinges for the +Y ExpSA wing (see Figure 3 for coordinate definition) that deployed it from the main solar array consisted of a standard spring hinge design, while the root hinges for the –Y ExpSA wing used two experimental EMC hinges that were designed and fabricated by Composite Technology Development. Details on the EMC hinge can be found in reference [7]. Once the deployment action initiated from the main solar array with the root hinges, the ExpSA wing then deployed using a combination of tape spring and a proprietary "living hinge" technology [2].

3.6 IV Box (current/voltage measurement)

The IV box served multiple functions that included: (1) switched the ExpSA wings from bus power mode to electrical characterization mode, (2) provided variable electronic load to characterize the electrical performance of the wings from open circuit to short circuit, and (3) heater control for the elastic memory composite hinge during deployment. The flight IV box is shown in Figure 7. The notional timing diagram is shown in Figure 8 (actual timing differed somewhat, but followed this approach). The IV box stepped through multiple, pre-programed fixed electronic loads that started at open circuit (zero current) and proceeded to short circuit (maximum current). Each electronic load condition was held for a fixed time, and the current and voltage were measured. The wing voltage was directly measured and the current was calculated based on measured voltage drop across a resistor placed in series with the wing electrical circuit. The resulting data set was a stair step down for voltage, and a corresponding stair step up for current. The IV Box outputted the measured values as analog voltages that were read by the main spacecraft avionics.

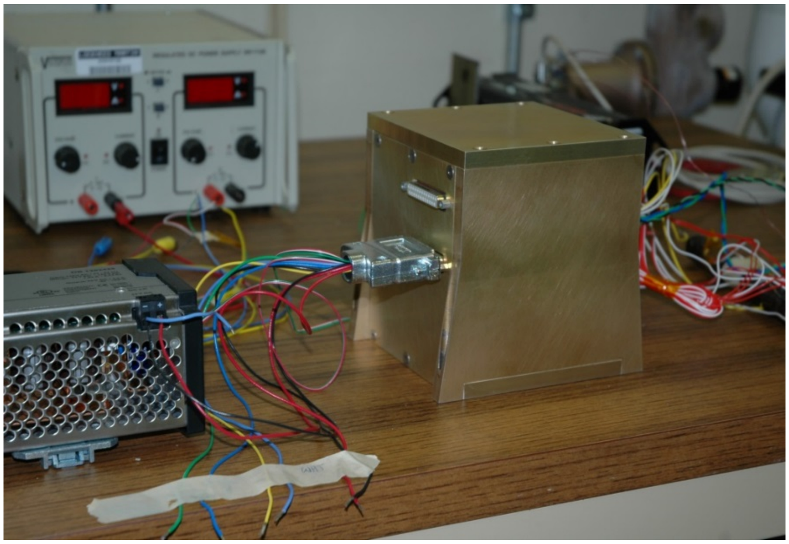

Figure 7. ExpSA IV Box

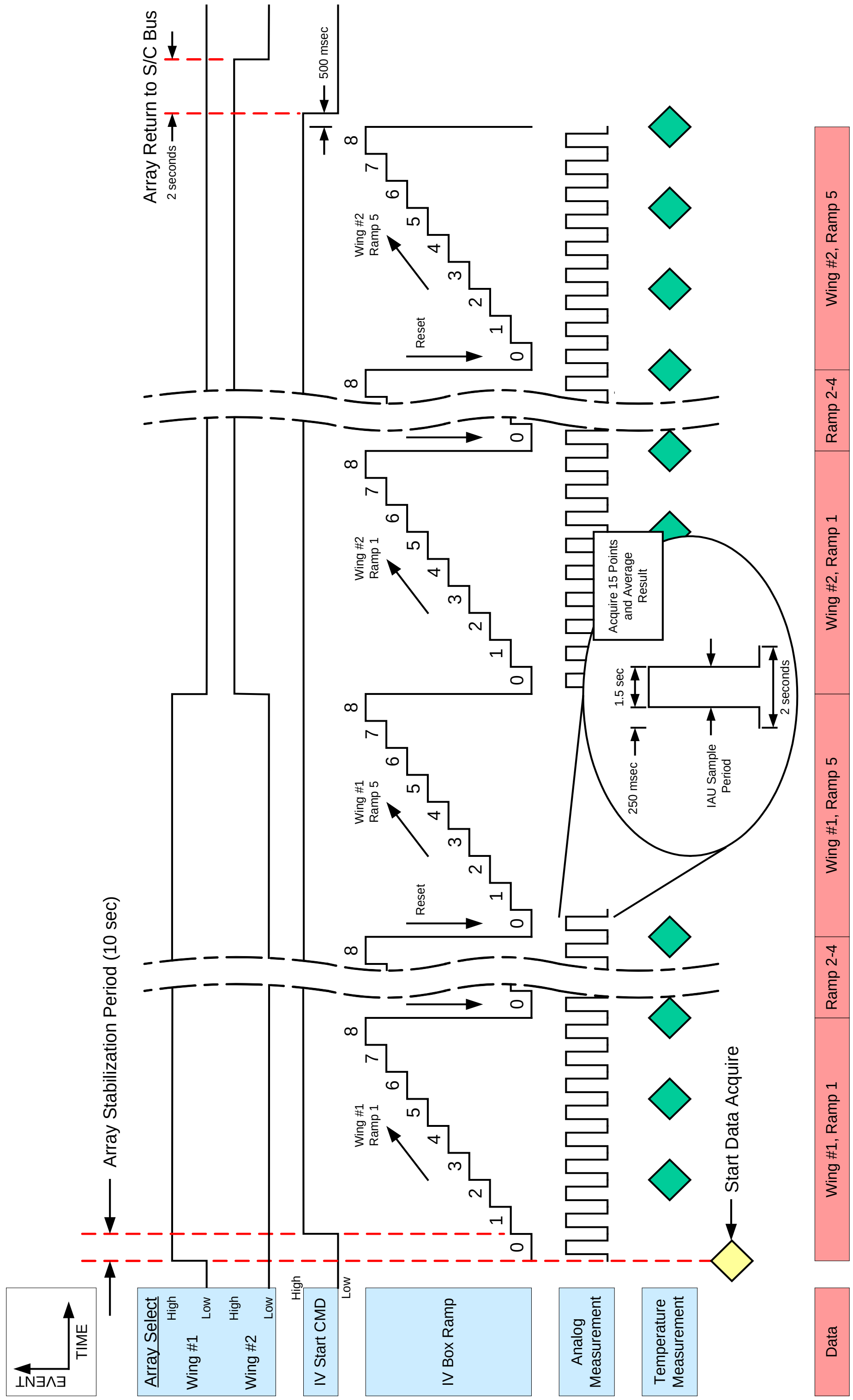

Figure 8. Notional IV Data Collect Sequence

4 RESULTS AND DISCUSSION

4.1 Pre-Flight Testing

Prior to launch, a suite of preflight space environmental testing was conducted. The testing included vibration, thermal vacuum, deployment, and electrical performance. A summary is included below, but complete details can be found in reference [1].

4.1.1 Deployment Testing

Deployment testing was conducted for each ExpSA wing. The ExpSA had three deployment stages. The first was the deployment of the root hinge, the second was deployment of the living hinges, and the final stage was deployment of the tape hinges. Deployment testing of each stage was performed independently, which isn't preferred, but was done for expediency sake. Ideally, deployment with a 0g offload system is the best approach, but was not possible within the resource constraints of this experiment. The resulting risk was deemed acceptable when balanced with resource allocation. Both wings were successfully deployed after all environmental testing.

4.1.2 Thermal Vacuum Testing

Thermal vacuum testing was conducted at the United States Air Force Academy (USAFA). Only the -Y wing was tested. The +Y wing was identical to the -Y wing, therefore it was accepted by similarity. The wing was cycled 4 times from -100 °C to 100 °C in a vacuum environment. The pre/post electrical testing of the wing showed no appreciable degradation due to the thermal vacuum cycling.

4.1.3 Pre-launch Electrical Performance Testing

Electrical performance testing was conducted using a terrestrial solar simulator (AM1.5 – Air Mass 1.5) at the National Renewable Energy Laboratory (NREL). The pre-launch AM1.5 test results from the NREL measurements for both the +Y and –Y wings are shown in Table 1 (V_{oc} is open circuit voltage, I_{sc} is short circuit current, FF is fill factor, V_{max} is voltage at maximum power point, I_{max} is current at maximum power point, and P_{max} is power at maximum power point). The full current/voltage curve for the +Y wing is shown in Figure 9. The +Y wing was the only wing that produced measurable power on-orbit.

Table 1. a-Si ExpSA Wing IV Performance Comparison (AM1.5, 25 °C)

Parameter	***a-Si (SN 001) -Y Wing***	***a-Si (SN 002) +Y Wing***
V_{oc} (V)	56.92	57.00
I_{sc} (A)	1.651	1.689
FF (%)	61	61.9
Efficiency (%)	6.11	6.63
V_{max} (V)	42.15	42.32
I_{max} (A)	1.36	1.408
P_{max} (W)	57.34	59.59

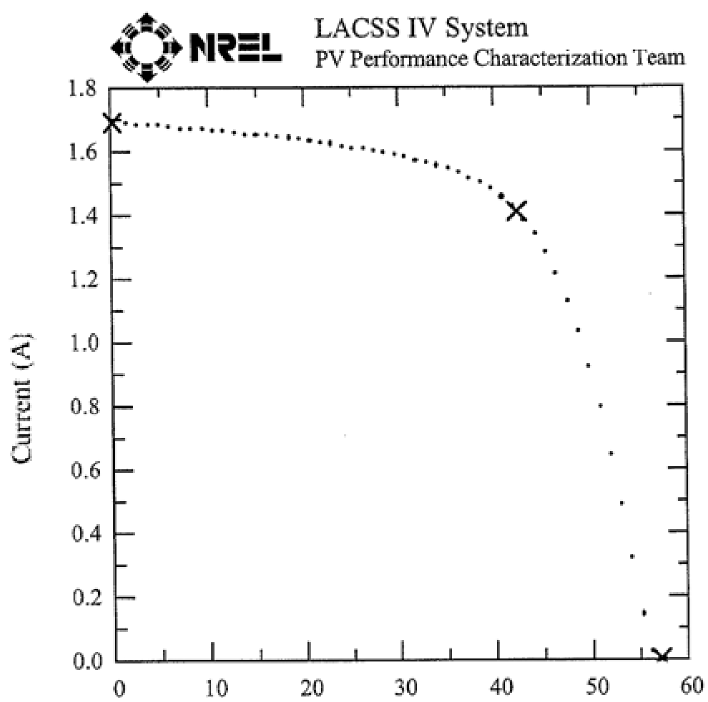

Figure 9. AM1.5 Pre-flight Electrical Performance of +Y wing (25°C)

Note: LACSS is Large Area Continuous Solar Simulator.

The performance of the solar array is dependent on the solar spectrum; therefore the electrical performance measured under AM1.5 was corrected to represent the expected performance under AM0. In estimating AM0 performance from an AM1.5 measurement, it is assumed that the voltage and fill factor are unaffected by the difference in illuminating spectrum. Further, for the triple junction a-Si solar cell technology flown, the top junction is the current limiting junction. Therefore the increase in output current is assumed to be a direct function of the change in current output of the top junction.

Subject to these assumptions, the expected initial on-orbit performance under an AM0 solar spectrum was estimated using a current multiplication factor derived based on the quantum efficiency data and the respective solar spectrums (AM1.5 and AM0)[1]. The expected initial on-orbit performance based on the preflight testing is shown in Figure 10.

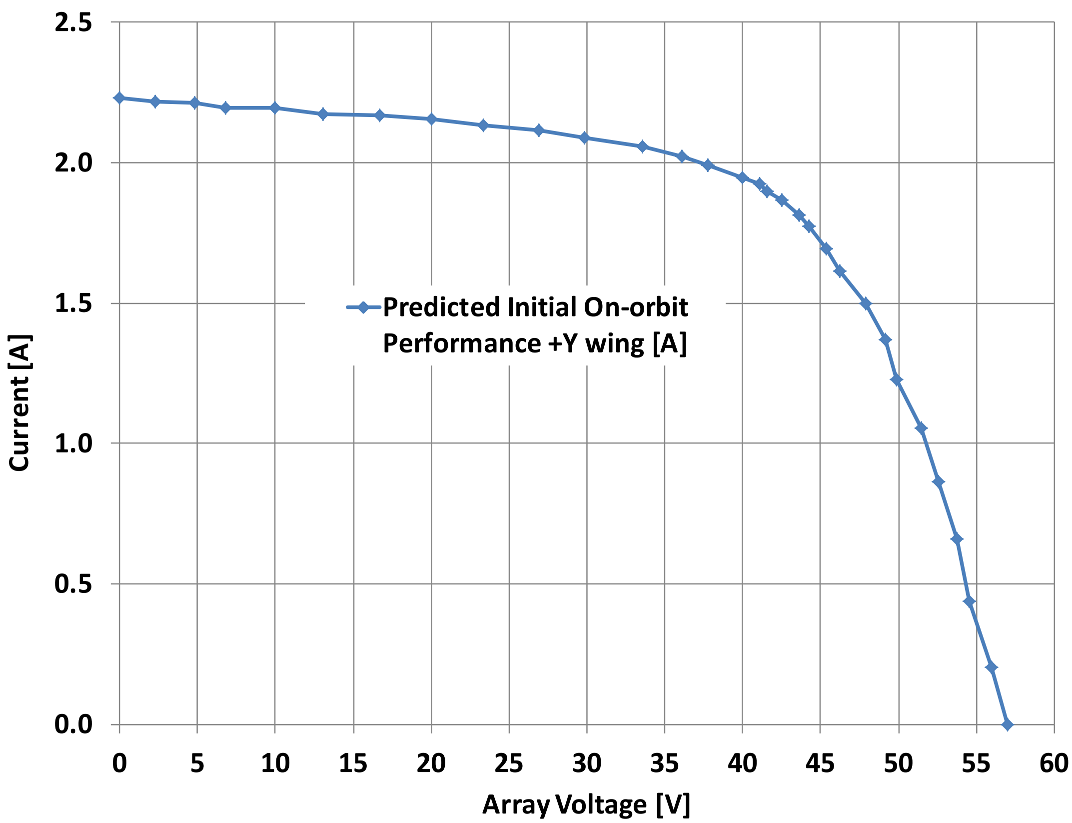

Figure 10. Predicted Initial AM0 Performance of +Y Wing (at 25°C)

[1] K. Beernink, United Solar Ovonic Corp, Personal Communication, Jun 2009.

4.2 On-orbit Performance

TacSat 2 was launched in December 2006, and the ExpSA was deployed soon after the main solar arrays were deployed. The first complete ExpSA data collect was conducted on 28 December 2006. Unfortunately, this revealed that neither the +Y or –Y wing were producing power. Additionally, analysis of the satellite telemetry revealed that the ExpSA wings were not providing power to the spacecraft bus during non-current/voltage measurement periods (bus power mode).

Optical imagery of the satellite revealed that the root hinge of the ExpSA –Y wing did not fully deploy (Figure 11). The –Y root hinge consisted of a set of two experimental elastic memory composite hinges developed by Composite Technology Development. While the reason for this failure is uncertain, two causes are speculated: 1) the designed deployment rate was not sufficient to allow unhindered deployment of the FITS system, which caused it to bind, and 2) the hindering torque imposed by the wiring harness that ran across the hinge line exceeded the deployment torque capability of the EMC hinges.

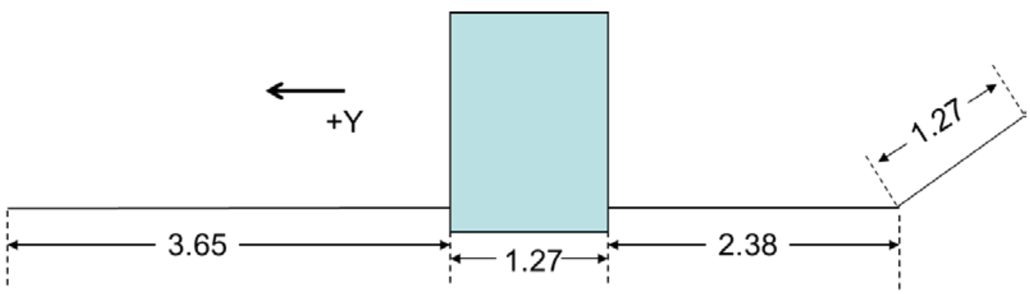

Figure 11. Stick-Figure Representation of TacSat 2 On-orbit Based on Optical Imagery

Note: Numbers in Figure 11 are arbitrary and approximate to show relative proportions.

Once the restraint panel was removed, the FITS system would have immediately started to deploy in concert with the root hinge. There were not coordinating deployment features to restrict the FITS until the root hinge was fully deployed. As such, it's possible that the deployment rate of the EMC hinge was not sufficient to allow the FITS system to deploy without hindrance, which could have caused the solar array to bind. Unfortunately, ground testing resource limitations (schedule/cost) prevented integrated, gravity off-loaded deployment of the integrated, full system (root hinge, y and z direction deployment). Instead, each deployment stage was independently ground tested. For a more complete discussion of this anomaly, please see reference [4].

Multiple electrical performance data collects were attempted during the month of January 2007. Unfortunately, both wings failed to output appreciable levels of power. Fortunately, another data collect was attempted in May 2007 and the ExpSA +Y wing was producing power, but did not provide power to the spacecraft bus. The –Y wing remained unresponsive throughout the duration of the TacSat 2 mission. All –Y current/voltage and temperature data sets are presented in the Appendix for completeness, as are the +Y data sets taken in Dec 2006 and January 2007 since neither provided usable current/voltage data.

Data obtained for the ExpSA +Y wing during May, June and July of 2007 are presented in Figure 12-Figure 19. In addition, the orbital temperature profiles of the main solar array wings and the ExpSA wings on 1 May 2007 are shown in Figure 20 and Figure 21. Each current/voltage set of the ExpSA wings is accompanied by the wing temperature during the current/voltage data collect.

Two temperature measurements sensors were mounted on the +Y ExpSA wing. However, data from ExpSA_PRT3 (+Y) were not trusted due to (1) non-physical response (choppy data with wide swings in output) and (2) out of family temperature levels. Therefore, for the electrical performance modeling of the ExpSA +Y wing, the output from ExpSA_PRT5 was exclusively used.

There was also a wide variation between the two ExpSA –Y temperature measurements. The data is relatively smooth from both the ExpSA_PRT4 and ExpSA_PRT6 sensors, and there is no reason to question the output values of either sensor. However, it is unlikely that the –Y ExpSA wing had an ~30 °C spatial temperature variation as the data indicate, even accounting for the possibility that one of the PRTs was mounted on a wing structural element versus on the Kapton® substrate. Given that the –Y wing was deployed at an approximately 45° angle, its solar flux was reduced (solar flux multiplied by cosine of 45°). Therefore, one would expect that the –Y ExpSA wing temperature would be lower than the ExpSA +Y wing temperature, which would indicate that ExpSA_PRT4 may be the most accurate.

The original design of the data collect was to perform 4 sweeps over the full current/voltage ranges, and to collect 8 data points per sweep. The approach taken was to use a constant current controller to set the electrical current value, maintain this value for a fixed time, and to measure the wing current and voltage during this duration. The IV Box measured the current and voltage of the wing at each data point, and outputted each as representative voltage that was then measured by two analog voltage channels on the main TacSat 2 bus. The analog voltage channels sampled at 10 Hz; therefore, each data point was held for a sufficient duration to ensure an adequate number of samples were obtained per data point. Two analog voltage channels were used to measure the wing voltage and current (conversion factor converted proportional voltage to the current measurement).

The first data set with measurable power output was taken on 1 May 2007 and is show in Figure 12, with the accompanying temperature data shown in Figure 13. The usable data can be seen in the regions of Figure 12 where there are voltage and current data points over a concurrent time span that are relatively constant. Unfortunately, while the original experimental plan was to measure 8 data points, an anomaly occurred that restricted the number of usable data points to two data points at intermediate load points, the open circuit voltage, and the short circuit current. Although substantial oscillations occurred as the electronic loading was reduced (higher current), the measurements obtained were actual current produced by the wing. Therefore, it was assumed that the short circuit current was represented by the highest measured current that occurred during the oscillations. One drawback to this assumption is that it is possible that the short circuit current was higher than the highest measured value. However, as will be shown later in this report, the on-orbit measured data subjected to this assumption shows good agreement with the predicted values obtained by applying known degradation factors.

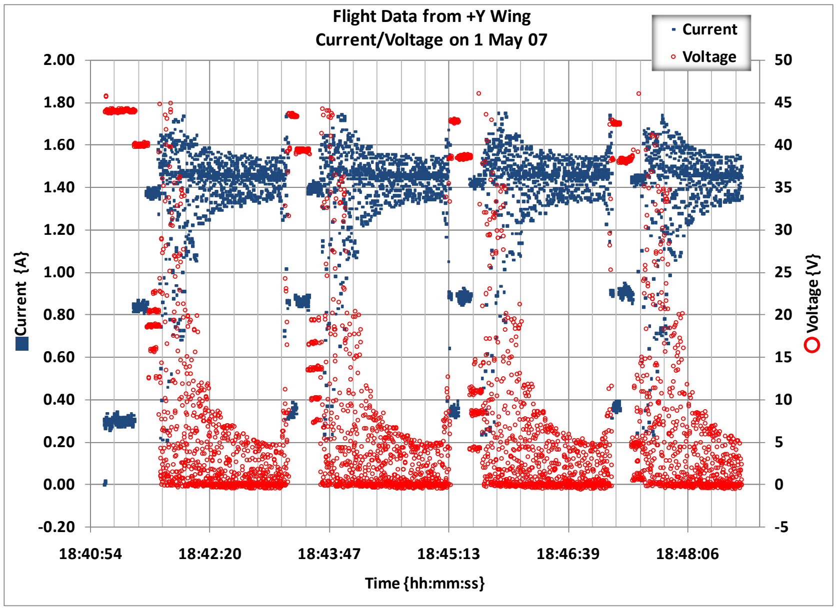

Figure 12. Flight Data from +Y Wing on 1 May 07 (Current/Voltage)

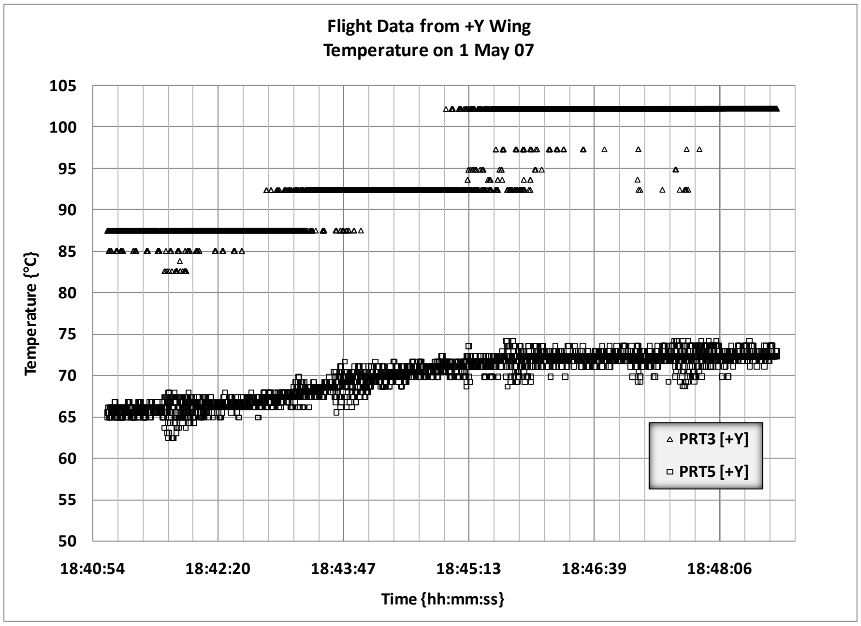

Figure 13. Flight Data from +Y Wing on 1 May 07 (Temperature)

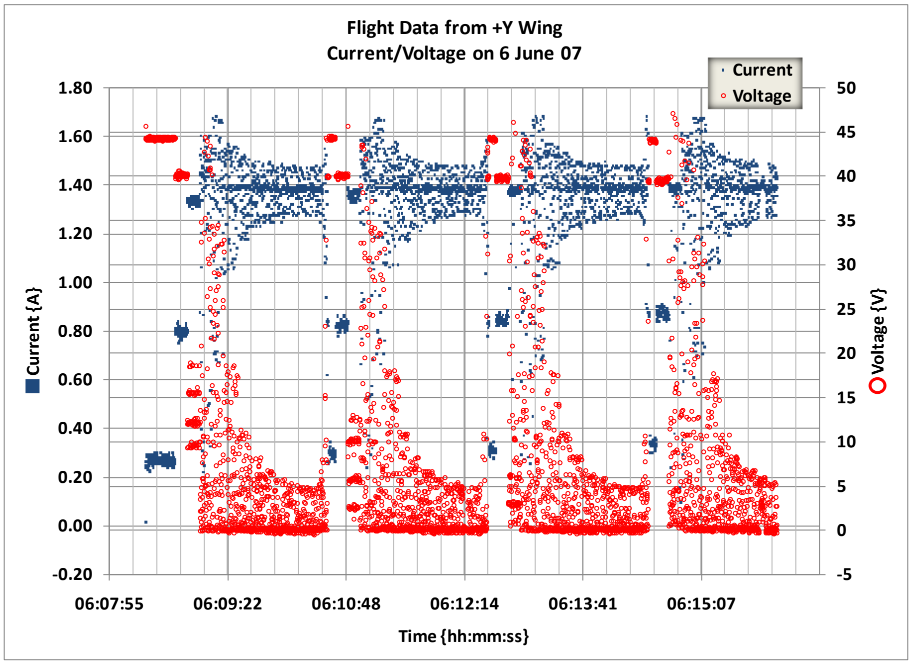

Figure 14. Flight Data from +Y Wing on 6 Jun 07 (Current/Voltage)

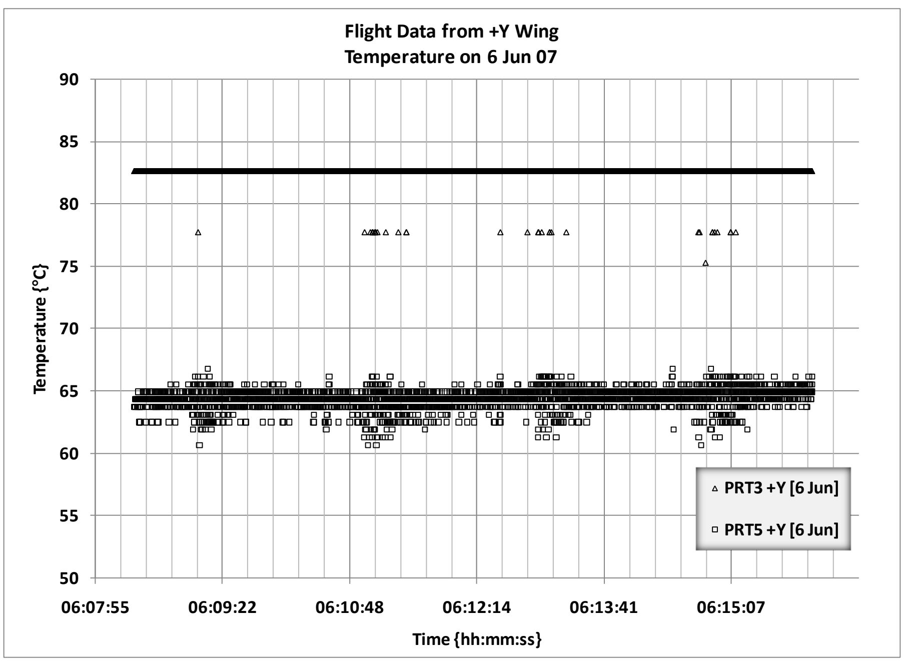

Figure 15. Flight Data from +Y Wing on 6 Jun 07 (Temperature)

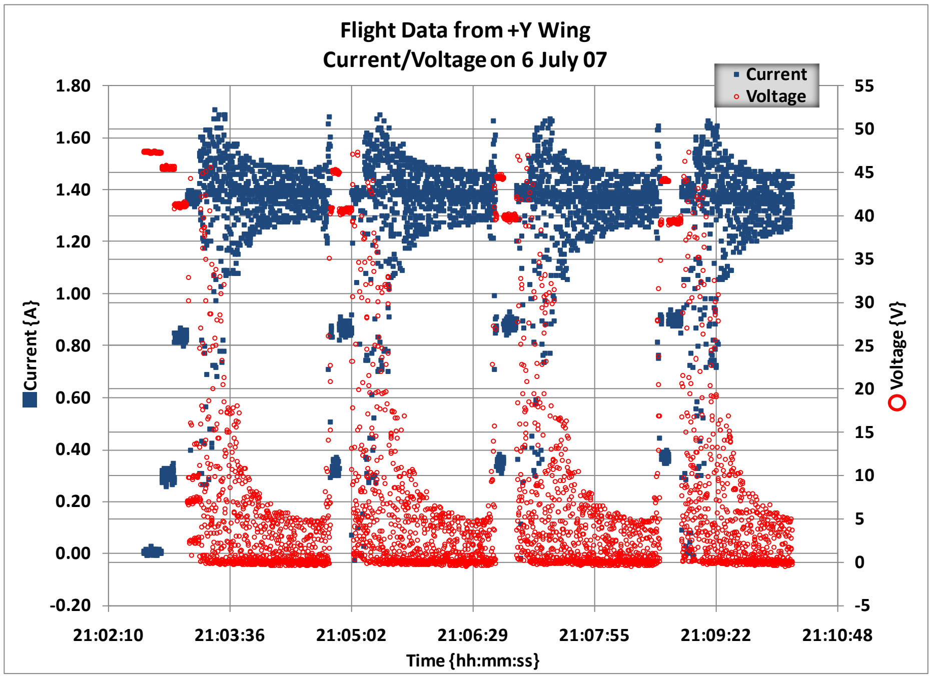

Figure 16. Flight Data from +Y Wing on 6 July 07 (Current/Voltage)

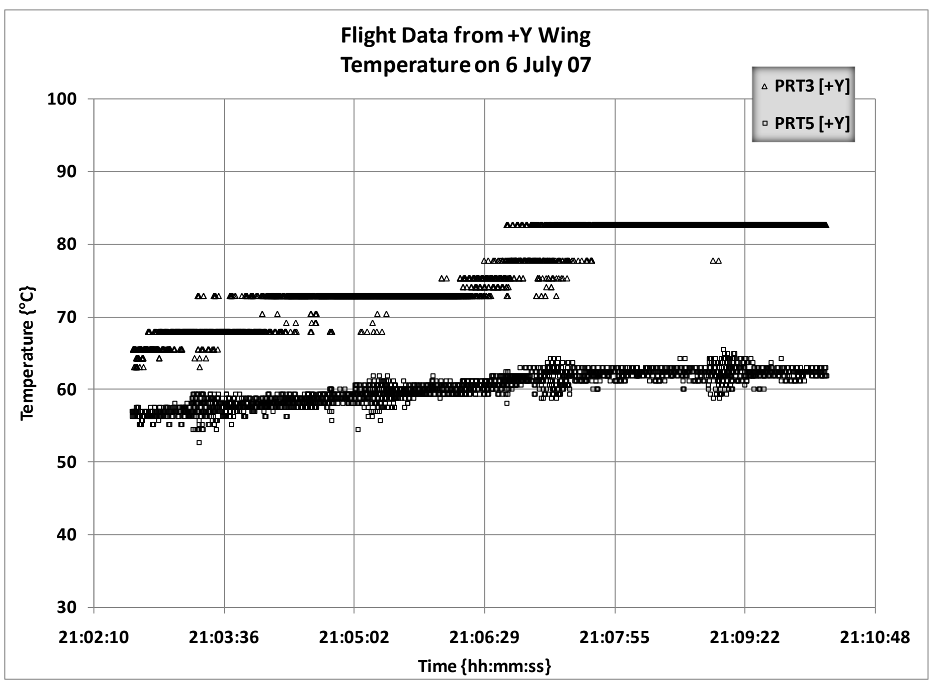

Figure 17. Flight Data from +Y Wing on 6 July 07 (Temperature)

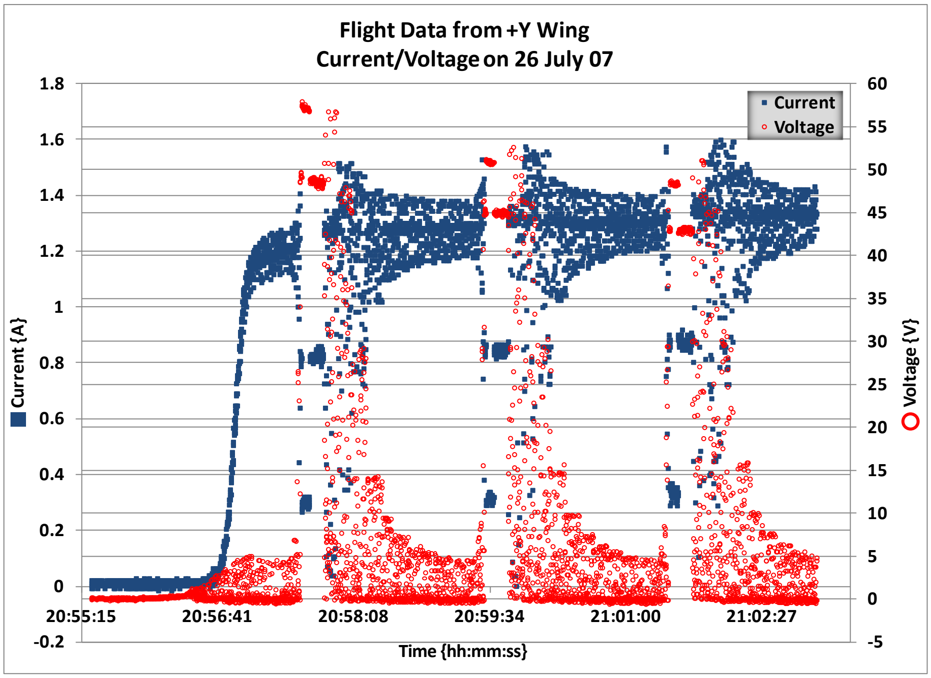

Figure 18. Flight Data from +Y Wing on 26 July 07 (Current/Voltage)

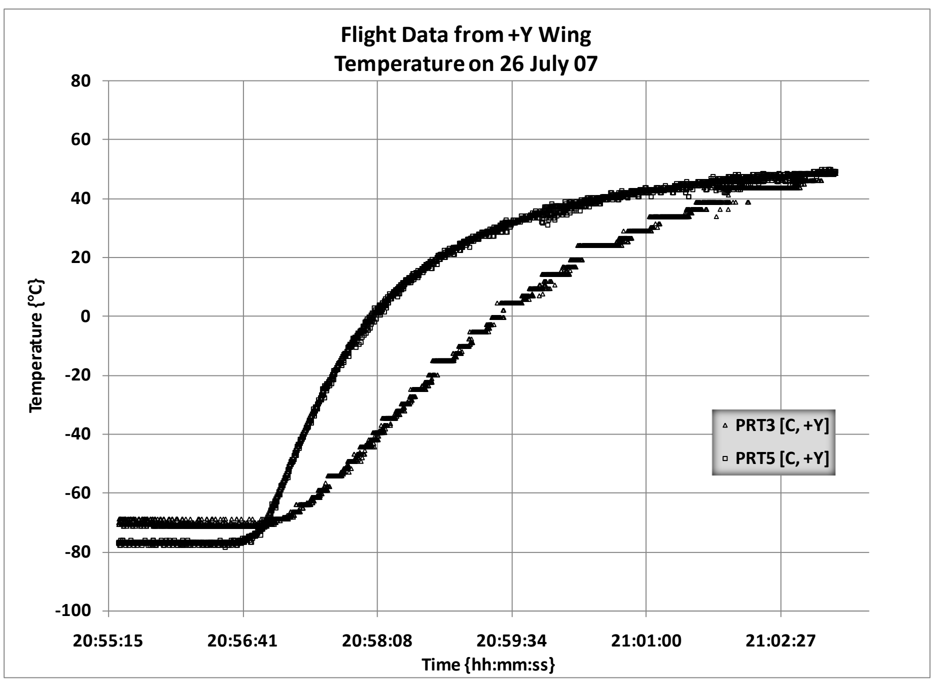

Figure 19. Flight Data from +Y Wing on 26 July 07 (Temperature)

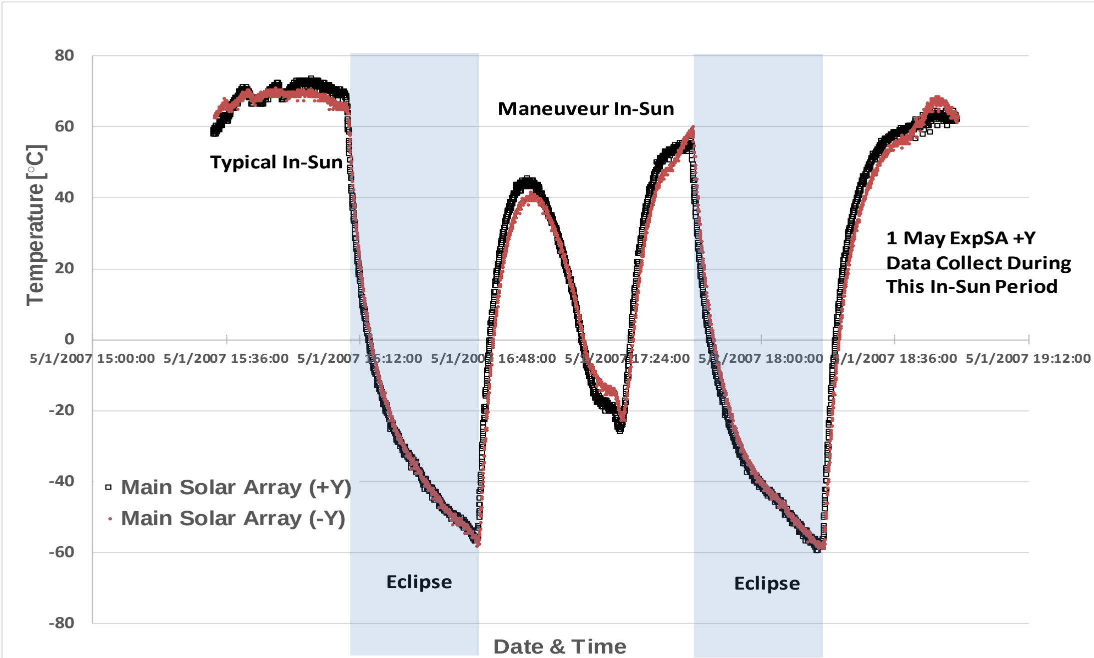

Figure 20. Main Solar Array Temperatures on 1 May 2007 (+Y and –Y)

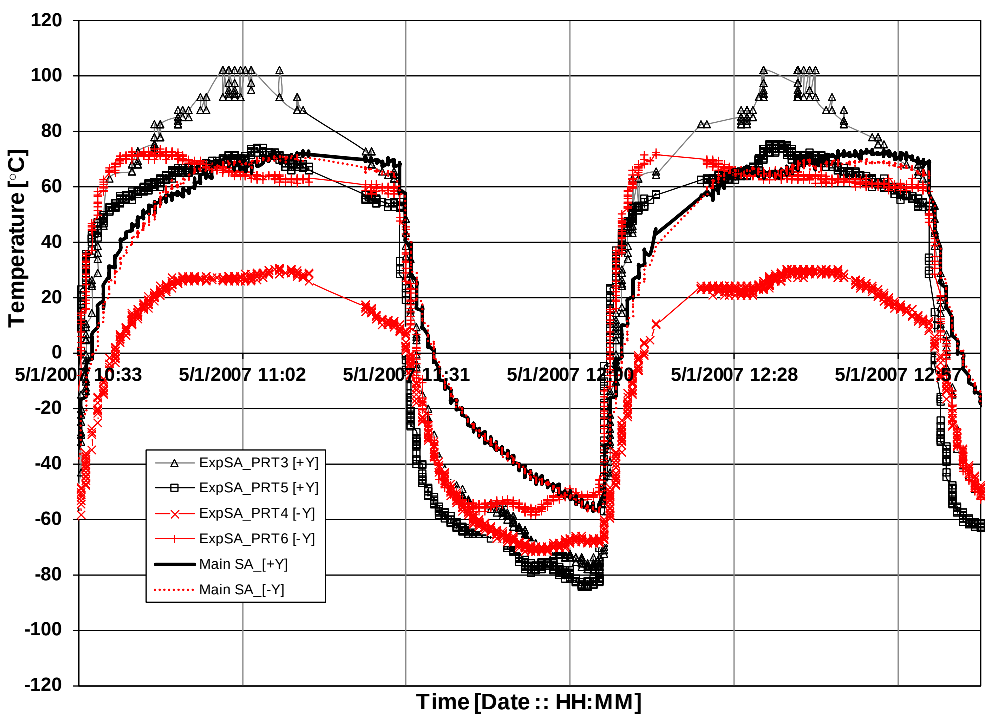

Figure 21. Example Orbital Temperature Profile (1 May 2007, ExpSA & Main Solar Arrays)

4.3 On-orbit Data Analysis

Degradation factors were used to predict the stable on-orbit performance. The degradation factors included reduction in voltage and current caused by the well-known a-Si Staebler-Wronski (SW) effect, and a current reduction caused by darkening of an experimental coating. The darkening reduction factor was estimated using ground data obtained by exposing the coating to ultraviolet (UV) radiation to ascertain the reduction in transmission [8].

The SW degradation varies with current and voltage. Measured SW degradation factors were available only at short circuit current, open circuit voltage, and the maximum power point[2] [3]. For comparison to on-orbit data, a full predicted current/voltage curve was needed. Therefore, it was assumed that the degradation factors varied linearly from open circuit to max power, and from maximum power to short circuit. This assumption was then used to generate SW degradation factors over the full span of the current/voltage curve.

The on-orbit predicted current/voltage curve (at 25 °C) was then calculated using the following expressions:

$$I_{predicted} = I_{AM1.5} * X * Y * Z_I \quad (1)$$

$$V_{predicted} = V_{AM1.5} * Z_V \quad (2)$$

Where $I_{predicted}$ is the predicted current value, $V_{predicted}$ is the predicted on-orbit voltage value, X is the AM1.5 to AM0 conversion factor and Y is the coating darkening factor. The SW degradation factors are denoted as Z_I (current) and Z_V (voltage). The numerical degradation values used are presented in Table 2. The resulting current/voltage curve is presented in Figure 22 as the predicted stable on-orbit performance.

Table 2. Solar Cell Degradation Factors

	AM1.5 to AM0[2] X	**Coating Darkening Y [8]**	**Staebler-Wronski Z [3]**
V_{oc} factor	1	1	0.960
I_{sc} factor	1.32	0.795	0.953
V_{max} factor	1	1	0.904
I_{max} factor	1.32	0.795	0.918

[2] K. Beernink, United Solar Ovonic Corp, Personal Communication, Jun 2009.

The measured on-orbit data points (corrected to 25 ˚C) are plotted in Figure 22 for comparison with the predicted, stable on-orbit values. The measured values are the average values during the first scan of each current/voltage measurement set obtained on that particular day (e.g. Figure 12). The correction to 25°C was made using measured voltage and current temperature coefficients for similar devices (α =-0.368 %/°C and β =0.1160 %/°C, respectively[3] using equations (3) and (4):

$$V(T_1) = V(T_2) * \left\{1 + \frac{(T_1 - T_2) * \alpha}{100}\right\} \tag{3}$$

$$I(T_1) = I(T_2) * \left\{1 + \frac{(T_1 - T_2) * \beta}{100}\right\} \tag{4}$$

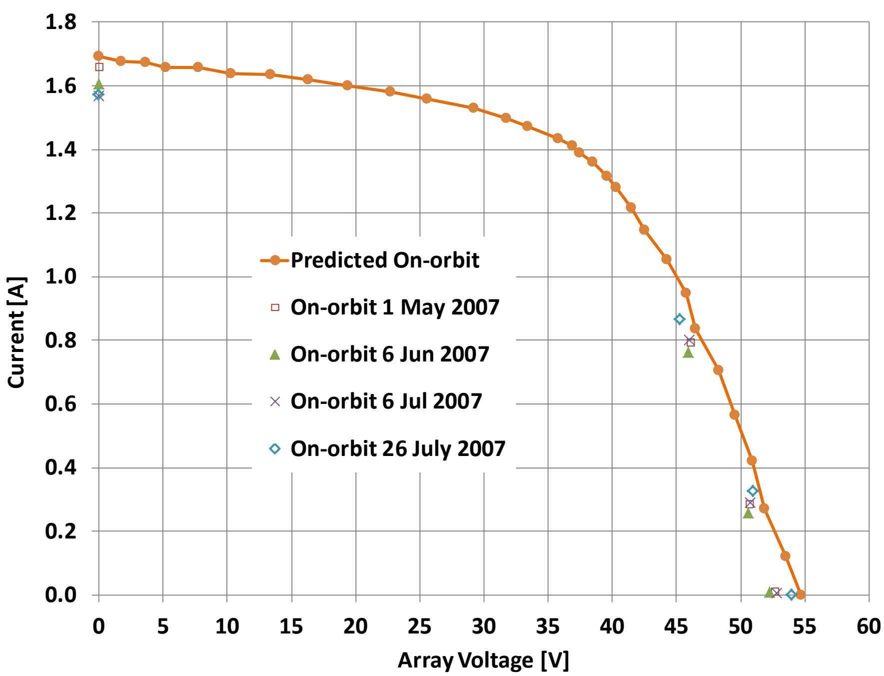

Figure 22. Comparison of On-orbit Data with Predicted Stable Current/Voltage Curve

The short circuit current (Isc) as a function of days on orbit is plotted in Figure 23. The measured Isc (corrected to 25 ˚C) is compared to the predicted initial Isc and the predicted stable Isc (both at 25 ˚C). The Isc appears to reach a relatively stable value that is slightly below the predicted stable value. Given the assumption made in extracting the short circuit current from the data, it is possible that the reported short circuit value could be less than the actual value (recall that the highest measured current was assumed to be the short circuit current during observed oscillations, see Figure 12). With this in view, the agreement between predicted and measured is very good.

[3] K. Beernink, United Solar Ovonic Corp, Personal Communication, Jun 2009.

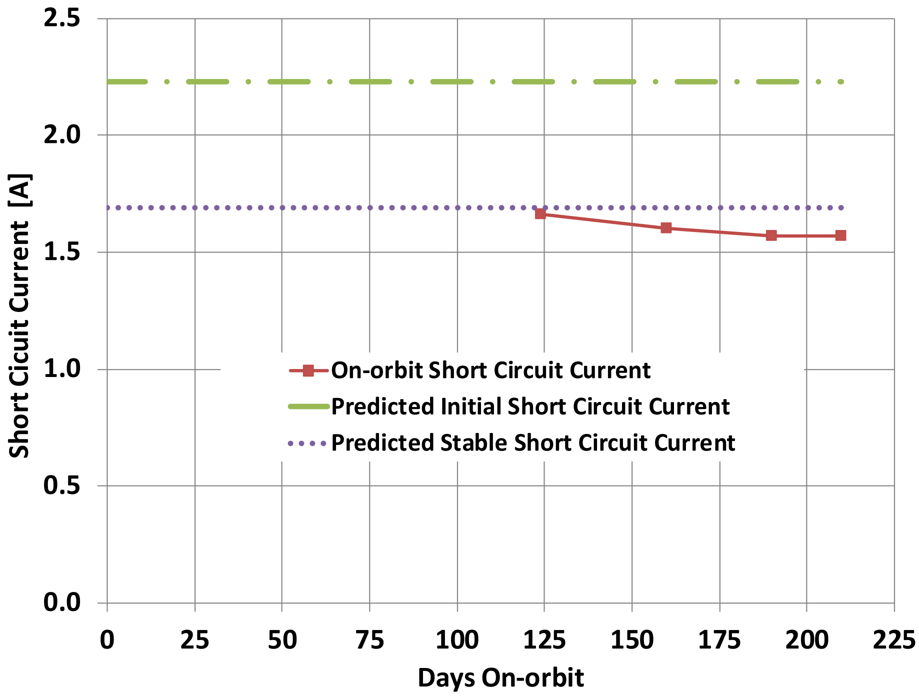

Figure 23. Short Circuit Current as a Function of Days on Orbit (All Corrected to 25 °C)

The open circuit voltage (V_{oc}) as a function of days on orbit is plotted in Figure 24. In addition, the predicted initial V_{oc} and stable V_{oc} are plotted for comparison. The V_{oc} appears to have slightly increased with time. However, it is likely that the variation is caused by uncertainty in the actual temperature of the solar cells. Given that the V_{oc} is highly dependent on temperature, relatively slight changes can impact it. Since the temperature sensor is on the back side of the array, there was a difference in the measured temperature and the actual solar cell temperature. This difference between the actual solar cell temperature and the measured temperature likely varied based on the orbital location due to thermal transient effects resulting from exiting the eclipse. With this uncertainty in view, the V_{oc} agrees fairly well with the predicted, stable V_{oc} and appears to be relatively stable over the ~80 days in which data was available.

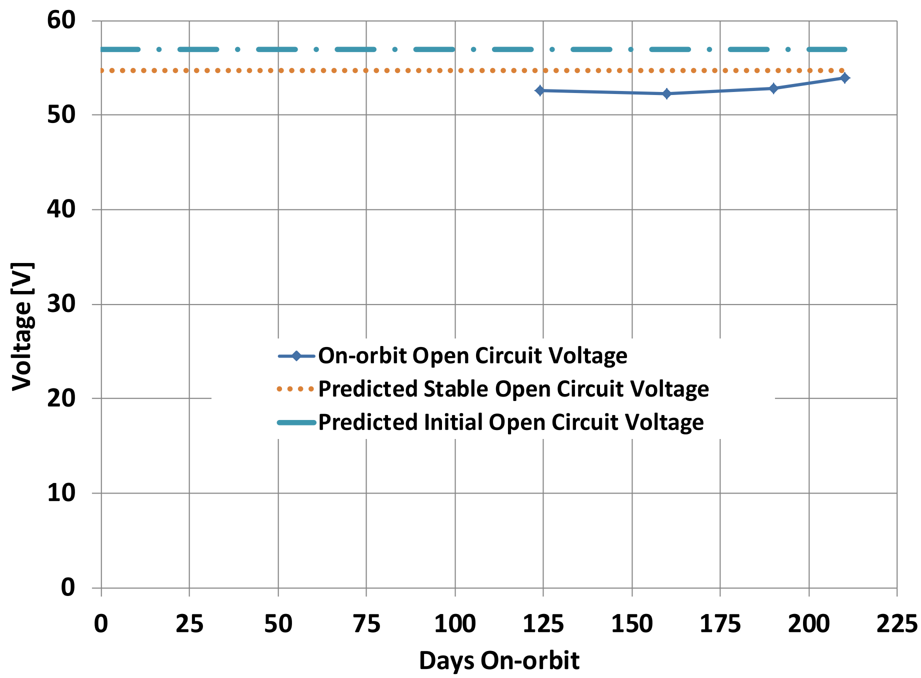

Figure 24. Open Circuit Voltage as a Function of Days on Orbit (All Corrected to 25 °C)

4.4 Root Cause Analysis for Lack of TacSat 2 Bus Power

Root-cause analysis was conducted in an attempt to identify the reason power was not provided to the TacSat 2 bus by the +Y wing. A cause and effect diagram (a.k.a fishbone) was constructed for this purpose (Figure 25). While a definitive conclusion could not be reached, two possibilities are highlighted: IV box malfunction and intermittent breaks in the copper electrical traces (array wiring failure). The main supporting evidence for intermittent breaks in the copper traces was obtained by examining an ExpSA EDU (engineering development unit) wing that did not fly. Multiple cracks in the copper traces were identified in the ExpSA EDU. The cause of the breaks was thought to be due to work hardening resulting from multiple bends that occurred during ground testing. This issue was remedied in future iterations of the technology by changing the copper alloy, establishing a maximum bending cycle limit, and design changes that limited the applied strain during stowage.

The IV box exhibited some measurement anomalies, and could have prevented power from being provided to the spacecraft bus. For this to occur, the cause would be a broken electrical connection, relay failure, or a commanding failure. Commanding was tested prior to launch, and the telemetry was examined to ensure correct commands were being issued on-orbit, so this is an unlikely cause. IV box relay failure or loss of electrical connection cannot be totally ruled out. However, the switching relays were redundant and mounted on opposing axes, which should have provided high reliability switching.

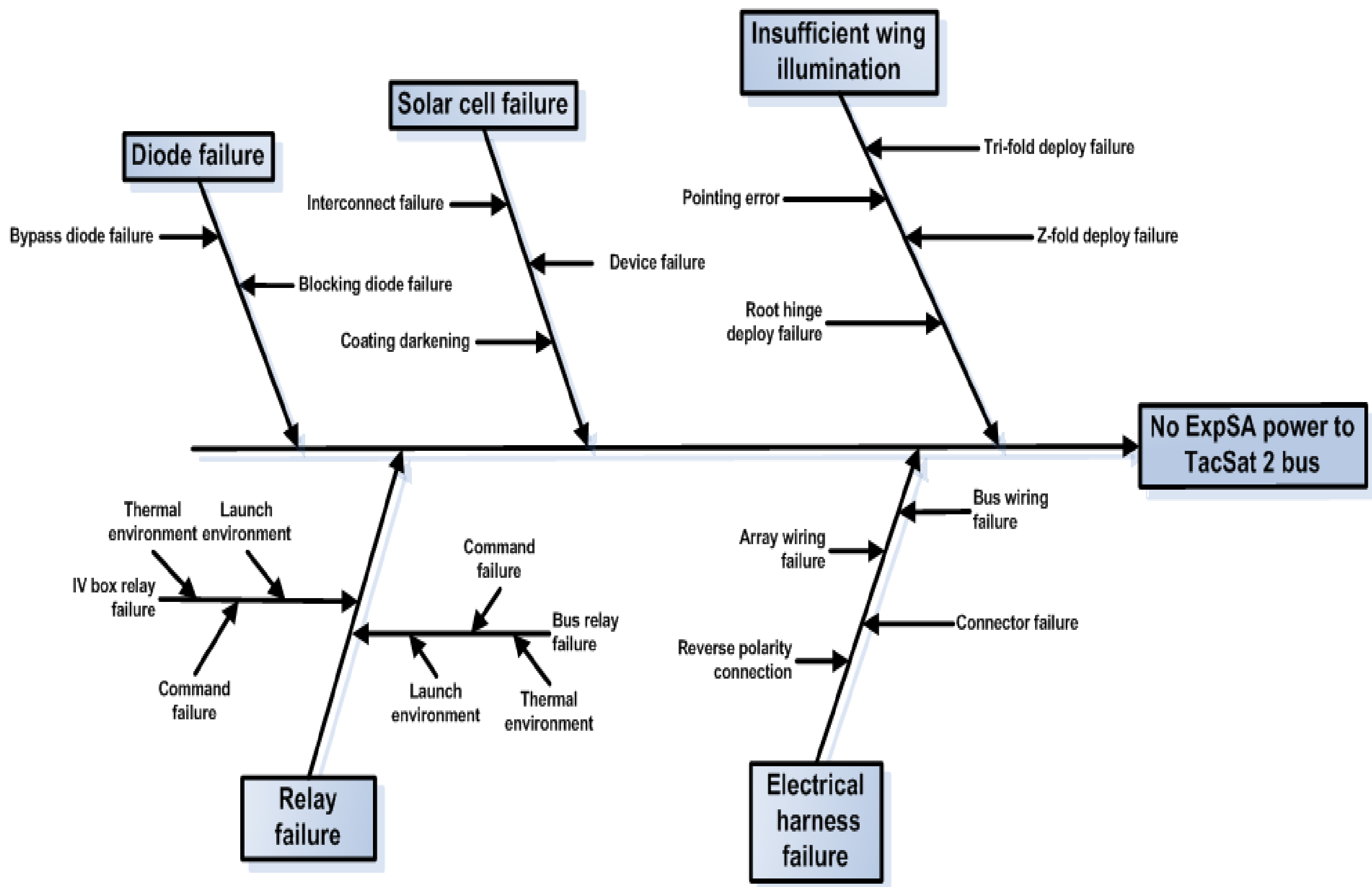

Figure 25. Fishbone Diagram Assessing +Y Wing Bus Power Failure

5 CONCLUSIONS

Of the four experimental objectives, two were fully satisfied. Successful deployment of the Fold Integrated Thin-film Stiffening solar array was demonstrated, fulfilling Objective 1. In addition, on-orbit electrical performance data was obtained for approximately 79 watts (BOL, AM0, 25°C) of triple junction a-Si thin-film solar cells integrated in a series/parallel configuration to support a 28 V spacecraft bus, which met Objective 2. Measured on-orbit electrical data showed reasonable agreement with predicted on-orbit operation. In addition, the electrical performance appears to have reached a stable operating point. The stable operation after 7 months in LEO (low earth orbit) and a close match to predicted operation bode well for potential use of a-Si technology in space. Objective 3 was not met as the EMC hinge did not fully deploy, which could have been due to a correctable harness configuration.

Finally, Objective 4 was not met as no evidence was seen in the spacecraft telemetry that either ExpSA wing was providing power to the electrical bus. Failure to provide power to the spacecraft bus could have been caused by a relay issue, or possibly due to intermittent electrical harness fractures that separated upon ohmic heating or other thermal transients. Spacecraft telemetry could not be comprehensively examined, so it is possible that ExpSA did provide current to the bus intermittently, but not at the times that the telemetry was examined.

The ExpSA experiment, while not fully achieving all objectives, was successful in advancing the FITS solar array deployment technology and the a-Si space solar cell technology. The flight experiment provided a relevant environment to test the integrated solar array system, and revealed some issues that were remedied with subsequent technology development. Also, since ExpSA was part of a larger mission and it was not the focus of that mission, priority was given to reducing spacecraft schedule and cost risk more so than additional ExpSA testing to verify all aspects of the experiment. Within these program constraints, the ground testing and associated risk profile were deemed consistent with the objectives, experiment complexity, and relatively low cost investment (i.e. return on investment was acceptable).

REFERENCES

[1] Enger, S. E and Gupta, N., *Modular Thin Film Solar Array for Responsive Space Missions*, AFRL-RV-PS TR-2008-1174, MicroSat Systems, Inc., Littleton, CO, DTIC, ADB346280, https://www.dtic.mil/DTICOnline/downloadPdf.search?collectionId=tr&docId=ADB346280, (Feb 2009.)

[2] Enger, S., Gupta, N., and Zuckermandel, B., *Electronic Devices – Foldable Integrated Thin-film Stiffening (FITS) for Spacecraft Electronic Solar Array Power Components*, AFRL-VS-PS-TR-2006-1164, MicroSat Systems, Inc. Littleton, CO, DTIC, ADB323490, https://www.dtic.mil/DTICOnline/downloadPdf.search?collectionId=tr&docId=ADB323490, (Nov 2006.)

[3] Guha, S. and Yang, J., *Ultra-lightweight High Efficiency Multijunction Thin Film Solar Cells for Space and Airship Applications*, AFRL-RV-PS-TR-2012-0136, United Solar Ovonics, DTIC, ADB385664F, https://www.dtic.mil/DTICOnline/downloadPdf.search?collectionId=tr&docId=ADB385664FA9453-06-C-0339, (Aug 2012).

[4] Hausgen, P. E., Carpenter, B., Gupta, N., and Turse, D., "TacSat 2 Experimental Solar Array On-orbit Data and Analysis," *Proceedings of the 43rd IEEE Photovoltaics Specialists Conference*, Portland, OR (2016).

[5] Hausgen, P. E., Granata, J. E., Tlomak, P., Jones, J., Enger, S., and Zuckermandel, B., "AFRL Thin-Film Photovoltaics DSX and Roadrunner Flight Experiments," *Proceedings of the 31st IEEE Photovoltaic Specialists Conference*, Lake Buena Vista, FL, pp. 614-617 (2005).

[6] Zuckermandel, J. W., Enger, S., Gupta, N. and Summers, J., "Modular, Thin Film Solar Arrays for Operationally Responsive Spacecraft," *IEEE Aerospace Conference*, Big Sky, MT (2007).

[7] Barrett, R., Francis, W., Abrahamson, E., Lake, M. S., and Scherbarth, M., "Qualification of Elastic Memory Composite Hinges for Spaceflight Applications," AIAA 2006-2039, *47th Structures, Structural Dynamics, and Materials Conference*, Newport, RI (2006).

[8] Sahlstrom, T. D., Hausgen, P. E., Guerrero, J., Howard, A. D., and Snyder, N. A., "Ultraviolet degradation testing of space protective coatings for photovoltaic cells," *Proceedings of the 33rd IEEE Photovoltaic Specialists Conference*, San Diego, CA (2008).

APPENDIX: FLIGHT DATA

Figure **Page**

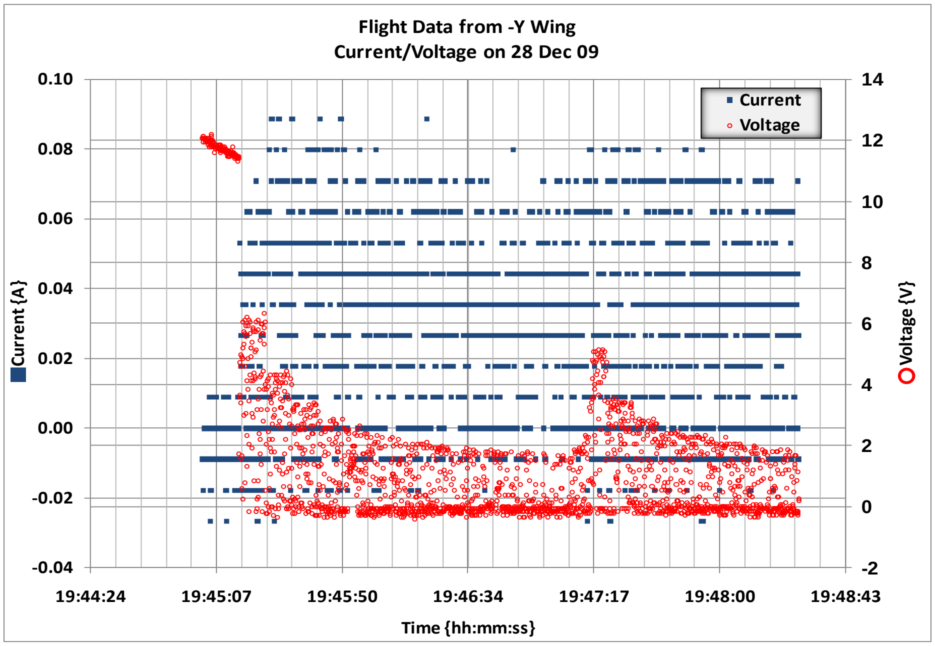

Figure A-1. Flight Data from -Y Wing on 28 Dec 06 (Current/Voltage)

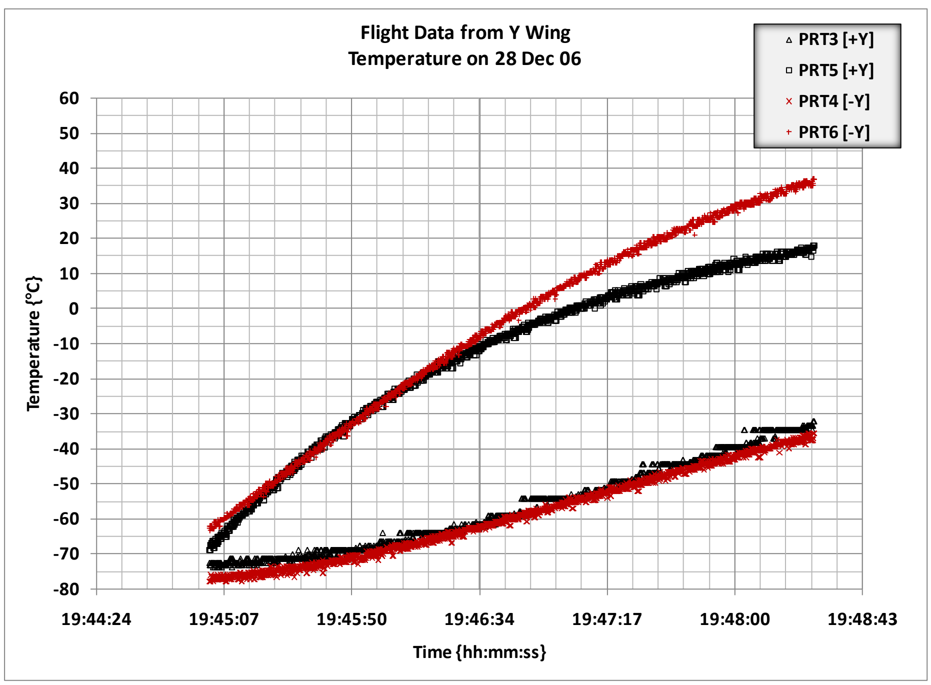

Figure A-2. Flight Data from -Y Wing on 28 Dec 06 (Temperature)

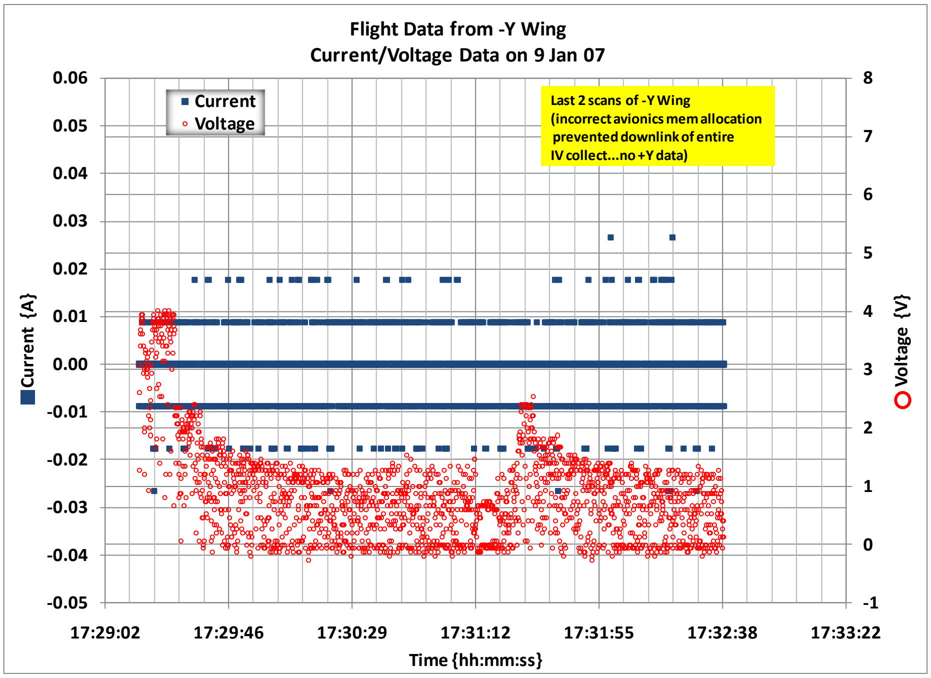

Figure A-3. Flight Data from -Y Wing on 9 Jan 07 (Current/Voltage)

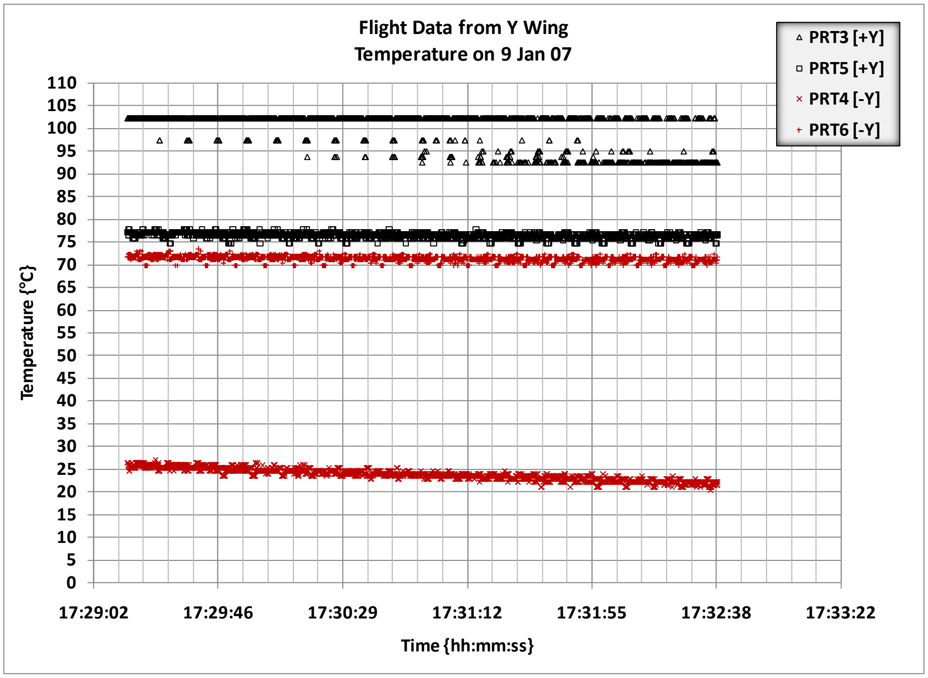

Figure A-4. Flight Data from +/-Y Wing on 9 Jan 07 (Temperature)

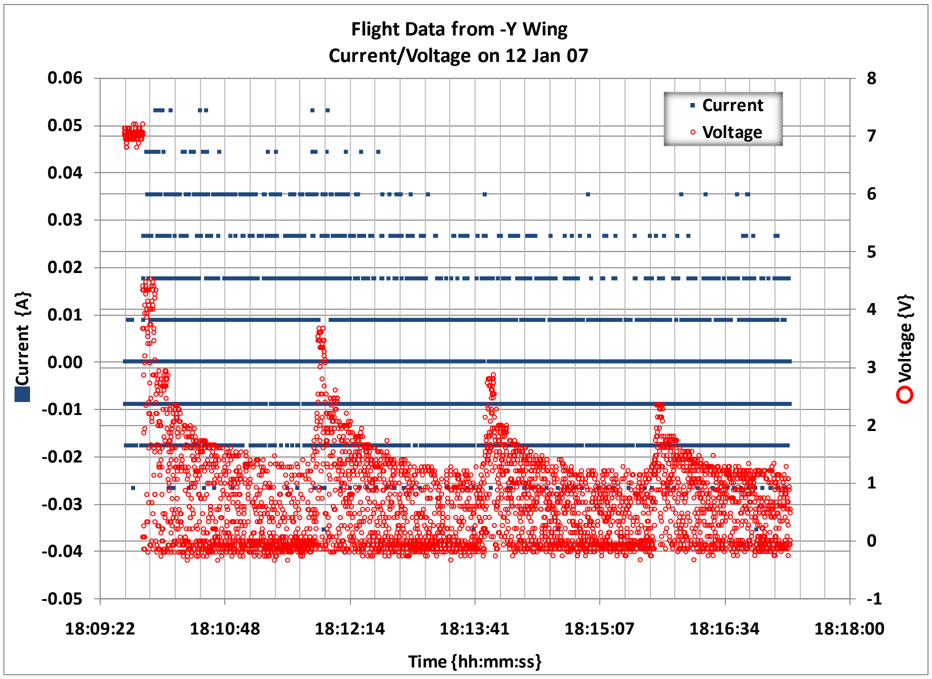

Figure A-5. Flight Data from -Y Wing on 12 Jan 07 (Current/Voltage)

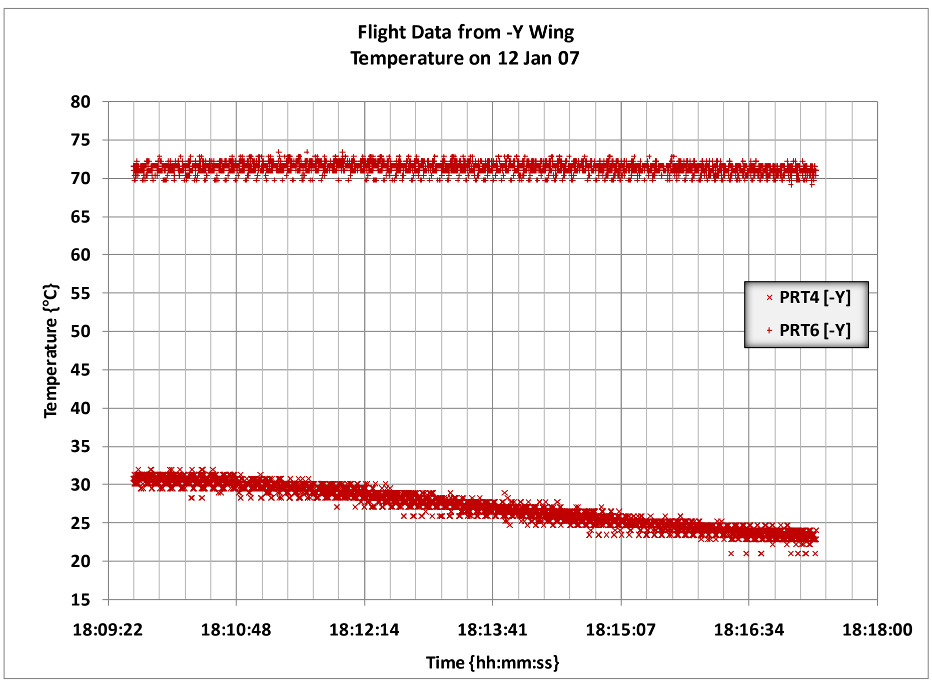

Figure A-6. Flight Data from -Y Wing on 12 Jan 07 (Temperature)

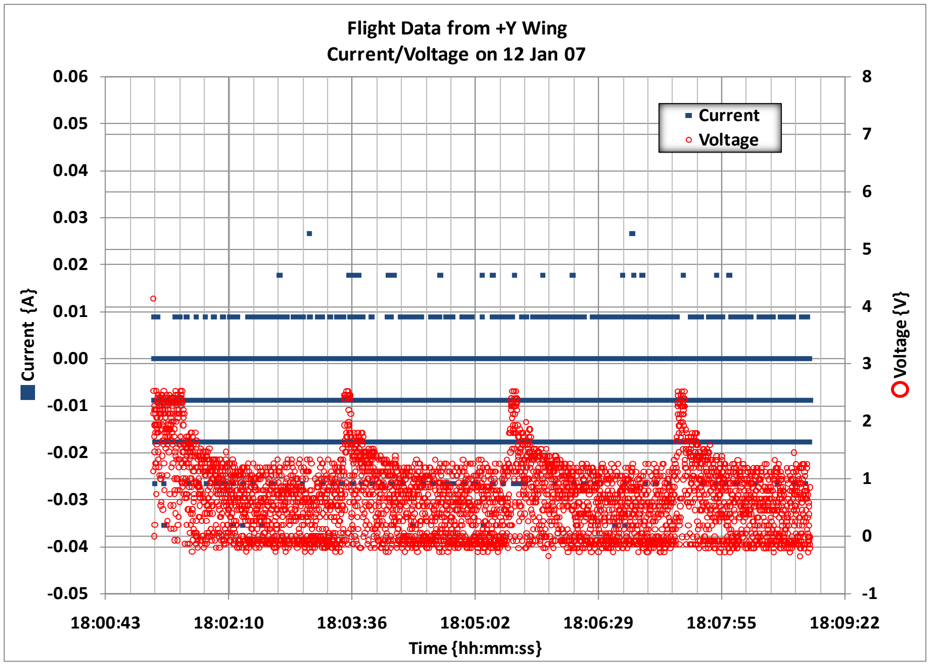

Figure A-7. Flight Data from +Y Wing on 12 Jan 07 (Current/Voltage)

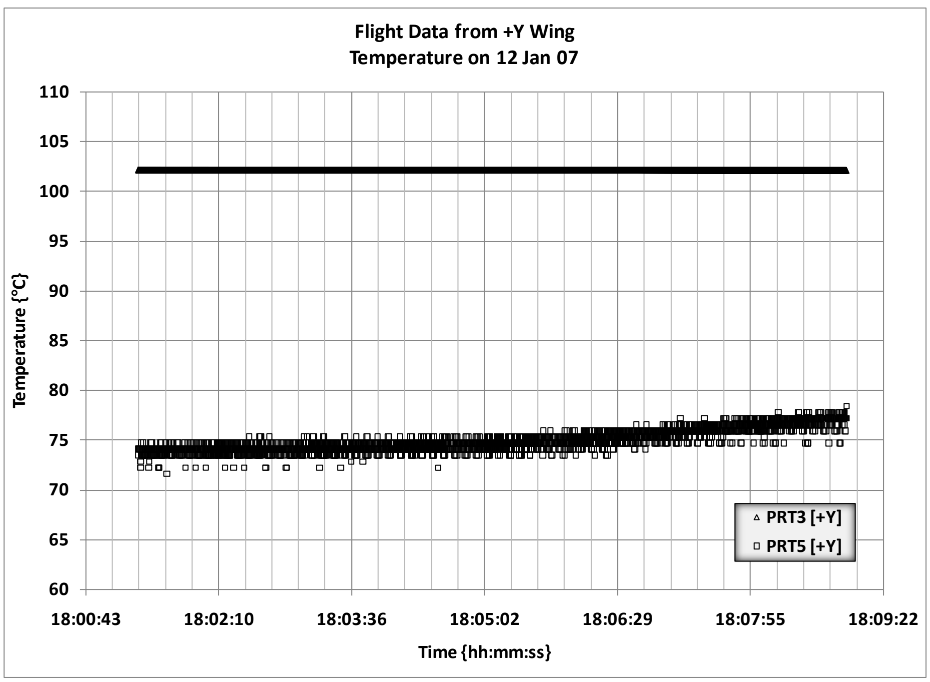

Figure A-8. Flight Data from +Y Wing on 12 Jan 07 (Temperature)

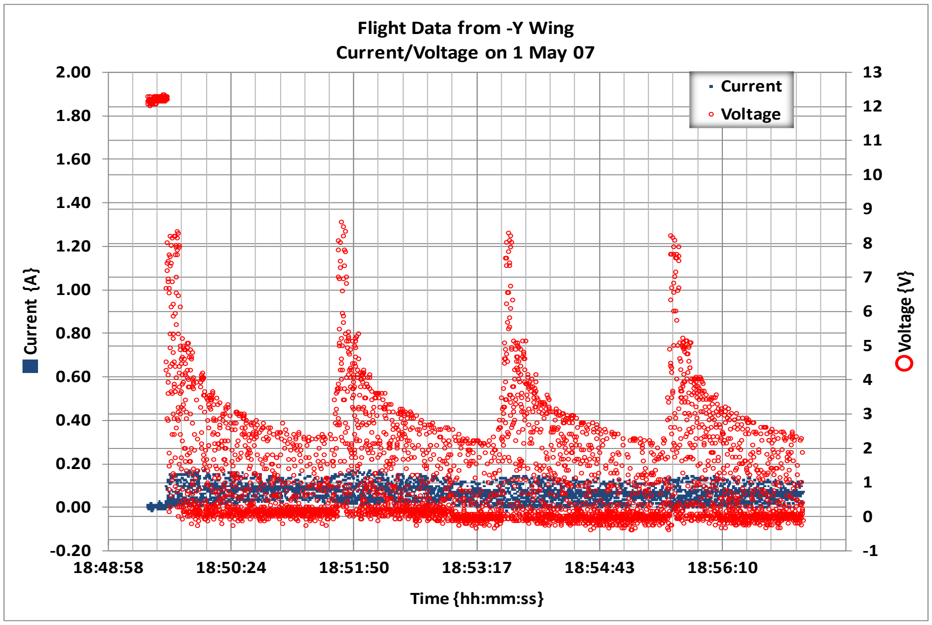

Figure A-9. Flight Data from -Y Wing on 1 May 07 (Current/Voltage)

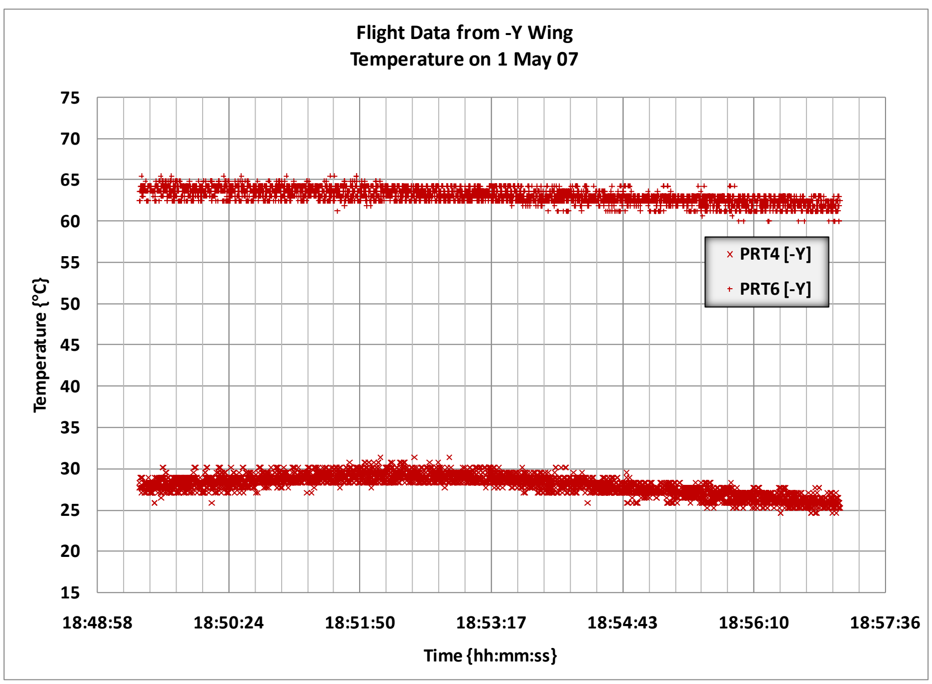

Figure A-10. Flight Data from -Y Wing on 1 May 07 (Temperature)

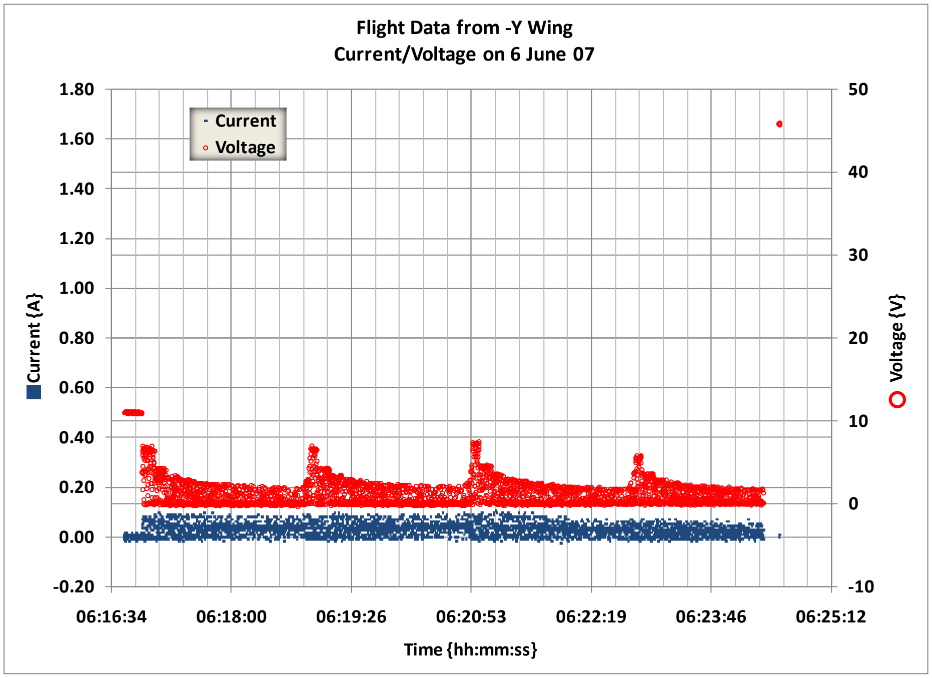

Figure A-11. Flight Data from -Y Wing on 6 Jun 07 (Current/Voltage)

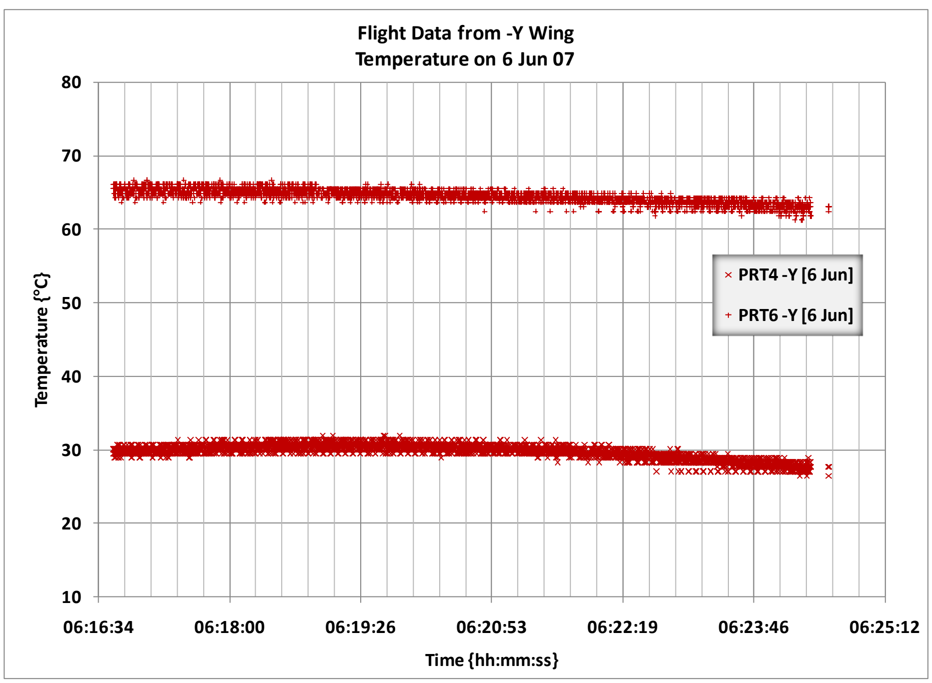

Figure A-12. Flight Data from -Y Wing on 6 Jun 07 (Temperature)

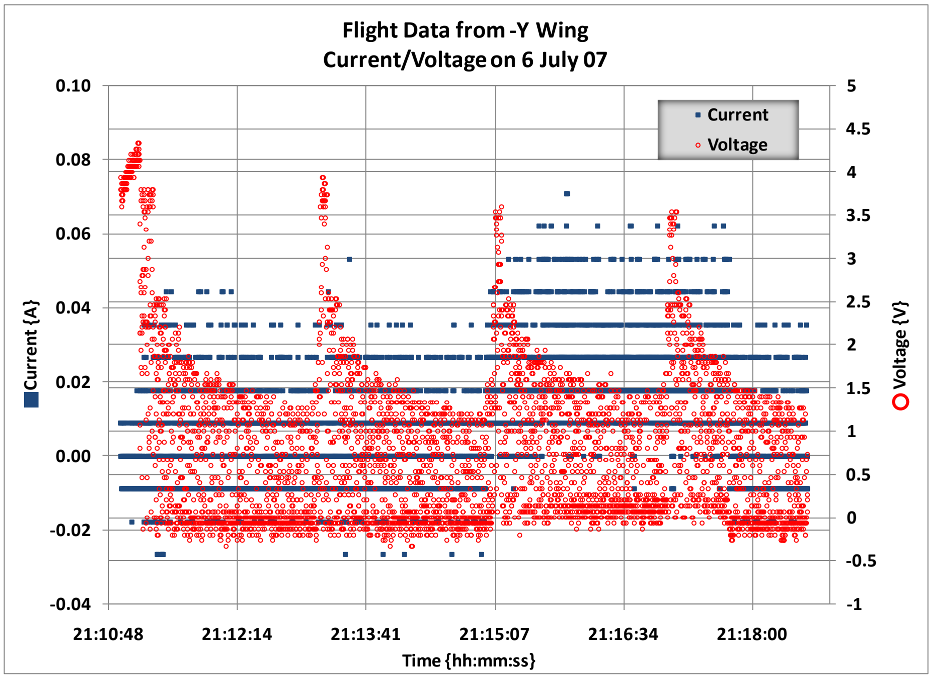

Figure A-13. Flight Data from -Y Wing on 6 July 07 (Current/Voltage)

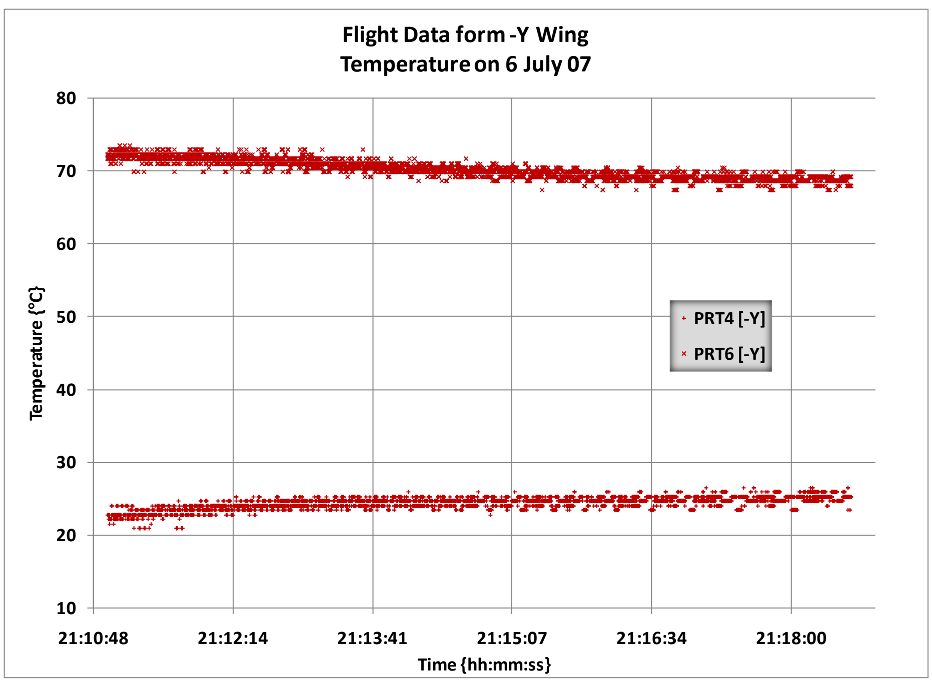

Figure A-14. Flight Data from -Y Wing on 6 July 07 (Temperature)

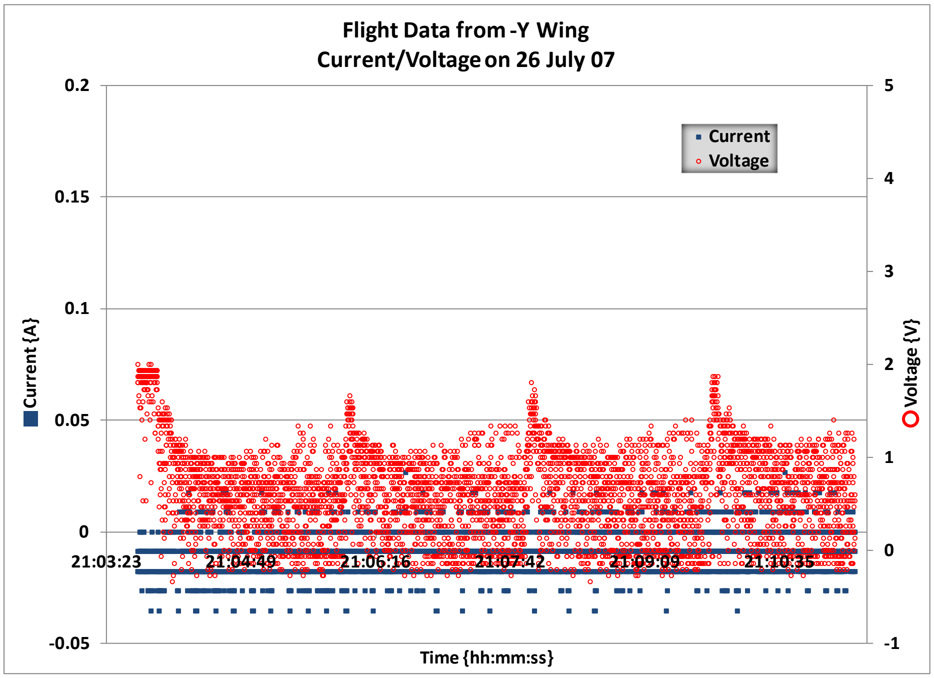

Figure A-15. Flight Data from -Y Wing on 26 July 07 (Current/Voltage)

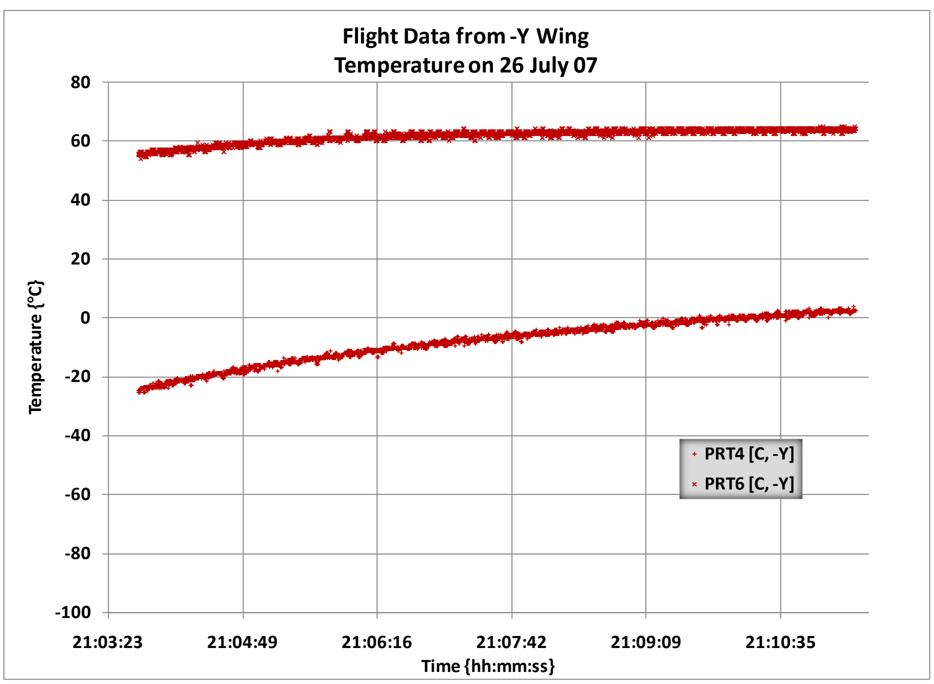

Figure A-16. Flight Data from -Y Wing on 26 July 07 (Temperature)

LIST OF SYMBOLS, ABBREVIATIONS, AND ACRONYMS

AM0	space solar spectrum
AM1.5	terrestrial solar spectrum
a-Si	amorphous silicon
BOL	beginning of life
CTD	Composite Technology Development
EDU	engineering development unit
EMC	Elastic Memory Composite
EOL	end of life
ExpSA	Experimental Solar Array
FF	fill factor
FITS	Foldable Integrated Thin-film Stiffening
IAU	integrated avionics unit
Imax	current at maximum power point
Isc	short circuit current
IV	current/voltage
LACSS	large area continuous solar simulator
LEO	low earth orbit
MSI	MicroSat Systems, Inc
NREL	national renewable energy laboratory
Pmax	power at maximum power point
PRT	platinum resistance thermometer
SOC	state of charge
SW	Staebler-Wronski
TFPV	thin-film photovoltaic
USAFA	United States Air Force Academy
USO	United Solar Ovonics
UV	ultraviolet
Vmax	voltage at maximum power point
Voc	open circuit voltage

DISTRIBUTION LIST

DTIC/OCP 8725 John J. Kingman Rd, Suite 0944 Ft Belvoir, VA 22060-6218	1 cy
AFRL/RVIL Kirtland AFB, NM 87117-5776	1 cy
Official Record Copy AFRL/RVSV/Paul Hausgen	1 cy